Escola de Camins
Escola Tècnica Superior d'Enginyeria de Camins, Canals i Ports
UPC BARCELONATECH

TREBALL FINAL DE MÀSTER

Títol

LATERAL STABILITY OF LONG PRECAST PRESTRESSED CONCRETE GIRDERS DURING TRANSIENT LOAD SITUATIONS

Treball realitzat per:

Fengbo Zhang

Dirigit per:

Albert de la Fuente, Antequera

Màster en:

Enginyeria de Camins, Canals i Ports

Barcelona, Junio de 2017

CONTENT

ACKNOWLEDGEMENT

I would like to express my sincerest appreciation to those people who helped me to accomplish this study.

Firstly and particularly, I would like to thank Professor Albert de la Fuente, who gave me this opportunity to work with him and has been supervising all my work during these 8 months. Every time when I felt confused and unconfident, he always showed me his positive attitude and encouraged me by all means. I was impressed by his passion and dedication to his work. What he shared with me about his professional experience will absolutely be helpful in my future professional life.

I would like to thank my supervisor Professor Feng Lin and our coordinator Jean from Sino-Spanish Campus in Tongji University, who offered me this opportunity to take part in this double degree program between Tongji University and UPC, especially the support from Professor Lin.

I would like to thank my dear colleagues from the same research group in Tongji University: Yanxiang, Jiayao, Wenming. Thanks for their help with my issues both in academic field and personal life. The first year working with them in Tongji was a valuable and unforgettable experience for me.

I would be grateful to my best friends I have met in Barcelona, Ling and Monica, who have always been with me during these two years. Thanks for their trust and company which have helped me get through many difficult moments.

My special thanks to my friends and flat mates: Yuexin, Yuan, Xijun, Di, Jin, Long, Ji, Fan, He. Though some of them are not living in Barcelona, their concerns for me from time to time are very important to me. It was very lucky to meet them and spend many happy moments together.

To those people whom I have met in the University and my language school: Rim, Mattia, Javier, Laura, Clara, Irene, Guilherme, Jono, Iva, Alba, Itamar.

Last but not least, my utmost appreciation to my dearest parents: Ji and Hengling. Their dedication to their work as being doctors and their attitudes towards our life teach me how to grow up and get independent. Thanks for all their unconditional support and encouragement, and mostly, trust for their daughter!

ABSTRACT

Since the invention of prestressing appeared, this technology has been widely used in civil engineering field. The combination of precast members and prestressing technics has been impelling the improvements in design methods, construction speed, structural performance and more importantly means of reducing cost over these years. Benefits of using precast prestressed concrete structures are easy to be found: reducing the structural deformation, using less steel material, increasing the capacity against cracking, fast speed and ease of erection, etc. Such structures are used in hydraulic structures, road structures, building structures and more commonly in bridge structures.

After the world's first precast prestressed concrete bridge was successfully built in Oued Fodda during year 1936-1937, many of such bridges has been constructed all around the world. Improvements in materials, advances in design method as well as technics have enabled the increase in the range of spans for precast prestressed concrete girders. However, the spans of girders are still under some limitations such as transportation requirements, erecting machine limits and more importantly the safety reasons.

Designers tend to pay more attention to the safety of structure during their service period. However, construction period is as much importance as service period for prefabricating structures. Many unexpected accidents have occurred during transportation and lifting phases of over these years. Not only will it influence the process of construction, but also increase the possibility of personnel casualty.

The objective of this research work is to investigate the factors which may cause the lateral stability problem of precast prestressed concrete girders during lifting. Based on the analytical model proposed by Robert Mast, a parametric study is carried out in order to obtain the possibility of stability failure in terms of different factors. The most important part of this research work is to build a reliable formula to evaluate the potential failure, which is only accessed through the designing information predefined for the girder such as the geometry of girder, sweep and strength of the material, etc. The formula will be validated by a real failure case and compared with the results from different provisions in current standards.

CHAPTER 1.

INTRODUCTION

1.1 BACKGROUND AND CONTEXT

1.1.1 Scope

As early as 1888, prestressing appeared along with the patented method for prestressing by engineer Doehring (Troyano, 2003). Prestressed concrete corbels were then built by Rabut, the mentor of Eugène Freyssinet who had a significant contribution to the development of prestressed concrete structures. It was Freyssinet who had firstly patented for the manufacturing process of prestressed concrete and put this invention into practice (Marrey and Grote, 2003). In 1933, three large prestressed concrete girders designed by Freyssinet had been inserted beneath a transatlantic quay in Leharve which was highly in danger of collapsing before being completed due to the neglect of silt beneath the gravel foundations. The successful application of prestressing concrete in the quay had impelled the further development of this technology. Moreover, Freyssinet had come up with ideas of precast prestressed concrete structures which had been applied in real projects in following years. For instance, during year 1936-1937, the world's first prestressed concrete bridge with 20-meter long and consisted of 4 bays with 12 precast girders was built in Oued Fodda, Algeria. Two years later in 1938, a span of 32 meters road bridge with four girders designed by Eugène Freyssinet was erected near Oelde (Beckum) (Marrey and Grote, 2003). During World War II, a bridge of a 42-meter span manufactured by precast elements was built across the river Klodzka Mysa during 1940-1941. (Marrey and Grote, 2003).

Many benefits of using precast prestressed concrete girders for bridges can be found from the view of design and construction. Bridges built by prestressed concrete girders have exhibited good structural performance and proven to be economical. For instance, using prestressing forces in beams can increase the beam's capacity against cracking. The precamber caused by prestressing forces may decrease the bending deflection of the beam during its service period. Moreover, less steel material is required in prestressed concrete structures. From construction point of view, the main advantages of using precast prestressed concrete girders widely in construction would be its fast speed and ease of erection. Therefore, more and more precast prestressed concrete girders are used in bridges during the last half century around the world. For example, the 60-meter long Luzancy Bridge built in 1946 in France and the 54-meter Walnut Memorial Bridge built in 1948 in Philadelphia, United States can be seen as milestones in this technology's development after World War II.

Unlike cast-in-place concrete structures, the precast elements should usually be prefabricated in factories and then be transported from the yard to the construction sites, along with being lifted onto their final positions and thus being integrated with other structural elements. Three important stages in the construction process are defined by Stratford and Burgoyne 2000: (1) transportation; (2) lifting and (3) placement in structure or temporary storage. Those three stages are illustrated in Figure 1.1, 1.2 and 1.3 respectively.

In recent years, the range of spans for precast prestressed concrete girders has been increased owing to the improvements in materials, optimized sections and other advances in design methods as well as technics. Long span girders exceeding 200ft (60.96 meters) are found to be used with optimized sections such as the California

Wide-Flange Girder and the Nebraska University (NU) I-girder (Cojocaru, 2012). More recently, a 223 feet long (67.97 meters) bridge with box sections were successfully installed in 2014 in the Netherlands.

However, girders are still used infrequently beyond a certain limit of span for several reasons, such as: (1) material limitations; (2) structural considerations; (3) size and weight limitations on girder shipping and handling, and (4) a general lack of information necessary to design and build longer spans (Castrodale and White, 2004).

Figure 1.1. Long precast prestressed I-shaped concrete girder during transport
Source: PCI Bridge Design Manual 2016

Figure 1.2. lifting of precast concrete girder for placement onto supports
Source: PCI Bridge Design Manual 2016

Figure 1.3. Precast concrete girders placed on bearings
Source: PCI Bridge Design Manual 2016

The increase in span would result in the increase in both the depth and the weight of girders. Meanwhile, the slenderness of the girder is inevitably decreased during this process. In some cases, in order to maximize the span range, the weight of modern beams has to be kept to a minimum value by reducing the width of the flanges. One possible consequence of this process would be the decrease in minor-axis bending and torsional stiffnesses compared to former sections (Herrando, 2015). In addition, the increase in weight and length of girders has made it more difficult to transport two or more girders like in the past, which let them to be cross-braced to each other. Girders with less torsional stiffness and more slenderness are more vulnerable to lateral instability during transient loading stages.

Usually, when girders are integrated with decks or columns, stability failure seldom could occur due to the inappropriate support. Moreover, according to design guidelines, designers tend to pay more attention to ensure the lateral stability of the finished structures. Nevertheless, precast prestressed girders are mostly prefabricated in factories and should be transported and installed at sites. The flexibility of support in those cases has made the lateral stability a problem become increasingly prominent. In recent years, there have been a number of accidents in stability failure during construction stages.

In 2013 in Portland's Marquam Bridghe, USA, an accident occurred while the girder was transported to the construction site. According to the traffic investigators, the trailer overturned due to the combination of brake on a sloping bend by the driver and camber of the road (see Figure 1.4). In 2004, a 45.7-meter long precast prestressed concrete bridge girder collapsed at the construction site in Pennsylvania (see Figure 1.5). Engineer suspected that additional sweep which may resulted from the sun heating on one side of the girder would have increased the

lateral instability potential since the eccentricity of the gravity load would apply torsion to these girders (Hurff, 2010).

Problem during lifting also appeared during the construction of a viaduct near to a town named Olost, in Catalonia, Spain. An small initial horizontal imperfection was measured in one of the precast prestressed concrete girders manufactured for the construction of the viaduct, which shifted the center of gravity of the girder laterally. However, the lifting process was permitted since this lateral imperfection was assumable according to the regulations for precast concrete elements. When the girder was lifted, it rolled sideways slightly due to this imperfection. A component of the self-weight load applied about the weak-axis then increased the lateral deflection. The beam was lowered down to examine the lateral deflection value. Cracks were found around the girder so it was replaced by a new manufactured girder. Figure 1.6 shows apparently the irreversible deformation of the girder (Herrando, 2015).

Figure 1.4. Accident during transpotation of a precast girder in Portland's Marquam Bridge, USA
Source: PCI Bridge Design Manual 2016

1.1.2 Previous research

From early 1950s, several studies have been carried out on stability problems of precast. Muller (1962) had put forward a method for calculating the critical vertical loads causing lateral buckling of a beam by considering different load types, positions as well as different cross section types. Based on Newmark's method, Swann and Godden (1966) have found a numerical method to determine the vertical load for buckling of a slender beam. Laszlo and Imper (1987) proposed reasonable values in terms of the factor of safety for different handling phases.

Furthermore, these authors also provided a way of enabling the stability of girders by using unbonded post-tensioned strands placed in the top flange or relaxation strands in a greased plastic tube being anchored at each end of the top flange. Mast (1989) had analyzed the mechanism of the lateral bending behavior by

considering the initial imperfection of the girder while lifting. This method had been extended to a more general way which can be applied both for transportation and lifting phases by Mast in 1994. Peart (1992) had concluded how the initial camber influence the buckling loads for the girders under different support conditions including simply support and hanging from cables at ends or a distance inward. It was summarized that the girder hanging from ends yielded the minimum buckling loads. When the lifting positions moved in from ends, the buckling loads can be increased as well. Stratford and Burgoyne (2000) mainly discussed the behavior of beams hanging from cables considering several situations: beams with inclined or vertical cables, with inclined or vertical lifting yokes, with lateral loads such as wind, with initial imperfections. The analytical solutions regarding lateral deflection were presented and compared with the results by using finite element method. More recently, Plaut and Moen (2013) derived a set of analytical solutions of internal forces, roll angles, deflections for the beam hanging from cables (Plaut et al., 2012; Plaut and Moen 2013) as well as unbraced beams on bearing pads (Plaut and Moen 2014).

Figure 1.5. Stability failure of precast prestressed concrete girders in Pennsylvania
Source: PCI Bridge Design Manual 2016

1.1.3 Regulations and standards

In current codes, detailed provisions regarding lateral stability of precast prestressed concrete girders during transient stages were rarely appeared. For examples, the PCI Bridge Design Manual defines the factor of safety which can be used to check the potential of stability failures of such beams. In the Spanish Structural Code EHE-08, maximum value for initial sweep is required. Though Eurocode 2 gives the acceptable conditions where ensure the lateral stability of such girders, it does not discuss about how to apply the detailed analysis if such conditions are not satisfied. Moreover, in some Chinese codes, construction regulations in terms of requirements of girder's size, ways of brace elements, strength of the material are presented, there are no specific formulas for examining the possibility of lateral stability failures of the girders.

Figure 1.6. Stability problem occurred during lifting in Olost, Spain
Source: PCI Bridge Design Manual 2016

1.2 MOTIVATION

During the last 50 years, many studies about lateral stability problem occurred in precast prestressed concrete girders during transient phases were carried out by several researchers. These studies were focused on analytical, numerical as well as experimental methods to better understand the lateral instability phenomenon and aiming at proposing general methods to cover the design. Even though some methods or analytical models were utilized in current codes, such as the model provided by Mast were used in PCI manual, stability problems still occurred in these years. Such failures would result in detrimental impact on several aspects: (1) extra economical loss due to the delay; (2) damages to construction equipment and, more importantly, (4) could endanger the lives of construction personnel. Therefore, it is of the utmost importance to study the reasons for such failures. Reliable means on evaluating the potential possibility of such failures and recommendations on improving the lateral stability are anticipated in deeper study.

1.3 OBJECTIVES

The **main objective** of this thesis is to propose a reliable formula for examining the possibility of lateral failure of precast prestressed concrete girders hanging from cables. This formula would include the geometric and boundary conditions of the girder as well as the mechanical properties of the constitutive materials.

This main objective is expected to be achieved by performing the following **secondary objectives**:

1. A deep revision of the existing models for dealing with the lateral instability design of precast prestressed concrete girders.

2. Develop a physical-based model to derive a design equation which includes the main variables that govern the problem.
3. Validation of the proposed formula by using other existing models and compare with real cases.
4. Study Case in which the suitability and reliability of the proposed formula is proven.
   Propose a set of conclusions and recommendations derived from the work carried out herein.

1.4 CONTENTS

This master thesis is divided in 5 chapters besides the present Chapter 1.

Chapter 2 presents the state of the art, which covers a general introduction to previous researches regarding lateral stability of the prestressed girders and provisions against stability failure of such girders in current standards.

Chapter 3 carries out a parametric study on how those factors influence the lateral stability of such girders. Those factors are: the length of the span, the strength of the materials, the initial sweep, lifting locations.

Chapter 4 presents a new approach for evaluating the possibility of lateral stability failure for precast prestressed concrete girders. Meanwhile, this approach is applied with sections from AASHTO and a real failure case to examine its reliability.

Finally, Chapter 5 presents the conclusions derived from the whole research work and future lines of research are suggested.

CHAPTER 2.

STATE OF THE ART

2.1 INTRODUCTION

Precast, prestressed concrete beams are widely used for bridges in constructions due to its significant advantage of construction speed. The advances in materials and precast techniques make the long-span precast prestressed concrete beams be possibly applied in many projects. When the span of beam is increased, the weight of the beam will be increased as well. The prestress will also be increased to enable its effectiveness. Many designers only consider the bearing capacity of the beam during their service period. However, the construction period which includes transport, stack, lifting etc. might be as important as the service period in prefabricated structures in terms of design. In temporary conditions, the self-weight is the main load during these processes and the minor stiffness is far smaller compared to the major stiffness and torsional stiffness. Usually, an initial imperfection is inevitable during fabricating which may result in an initial unbalance state during transport or lifting process. Moreover, the lack of sufficient lateral support in these processes makes the beam be more vulnerable to lateral instability under self-weight. Thus, the lateral stability problem of such beams has become a remarkable issue during transient load situations. Researches regarding the instability during lifting and provisions in current codes or guidelines are shown in the following part.

2.2 LITERATURE REVIEW

2.2.1 Researches on lifting problems

Robert F. Mast, 1989

Mast assumed that once the beam was integrated with the floor or the deck, the lateral instability of the beam would not be a problem. The integration of the structure can provide sufficient support to prevent the beam from lateral buckling. Mast also argued that in most textbooks the formulas for designing beams against lateral buckling were not adequate to deal with problems during transient stages such as transport on "springy" supports or lifting by cables (Mast, 1989). Two parts of the research performed by this author were focused on such problem. In part 1, he mainly discussed about the lateral bending instability of beams during lifting stage. In part 2, he extended the method to a more general case which the beam could roll down due to the elastic restraints.

In part 1, the basic assumption of his research was that the torsional stiffness of the beams which were hanged from flexible supports such as lifting loops was much larger than the roll stiffness. When the beam is lifted by flexible cables, it will be more easily to roll sideways. The rotation center of the beam is usually the location of the flexible supports on the beam. In lifting cases, the horizontal line passing through two cable loops on the top of the beam can be seen as the roll axis (Figure 2.1a). If the beam is perfectly and symmetrically built and the lifting loops are located at the center of the top flange without any eccentricity, the beam will be lifted plumb without rolling. However, in real cases, the sweep tolerance and lifting loop placement tolerances will always exist and result in the center of gravity of the beam moving slightly to one side of the roll axis. Therefore, the beam will tip about the roll axis at an initial angle θ_i due to the imbalance state, which further results in a component of the

weight of the beam $w\sin\theta_i$ (Figure 2.1b) applied about the weak axis and the increment in the initial roll angle θ_i. The component of weight applied about the weak axis will then cause a lateral deflection of the beam. The equilibrium state of the beam will be reached till the center of gravity of the beam vertically under the roll axis at an angle θ slightly larger than θ_i. Or the beam can also be damaged where the lateral bending is larger enough to fail the beam before reaching the equilibrium. Thus, in order to analyze the equilibrium state of the beam, the key point is to obtain the equilibrium angle θ. The final equilibrium state of the hanging beam can be illustrated in Figure 2.1b. It is assumed that the beam is uniformly tipped at an angle θ. The component of the weight applied on the weak axis is $w\sin\theta$ while the other component $w\cos\theta$ applied on the strong axis. As it is discussed before, $w\sin\theta$ has caused an additional lateral deflection $\bar{z}$ of the center of gravity of the deflected beam (Mast, 1989). To obtain the angle θ, $\bar{z}$ must be found first. Meanwhile, $\bar{z}$ results from the weight component $w\sin\theta_i$ which is applied about the weak axis. To make it more clear, $\bar{z}$ and θ are two interactional parameters which the one is dependent on the other. In Mast's research, he put forward a method to solve this problem. The procedure is explained as follows.

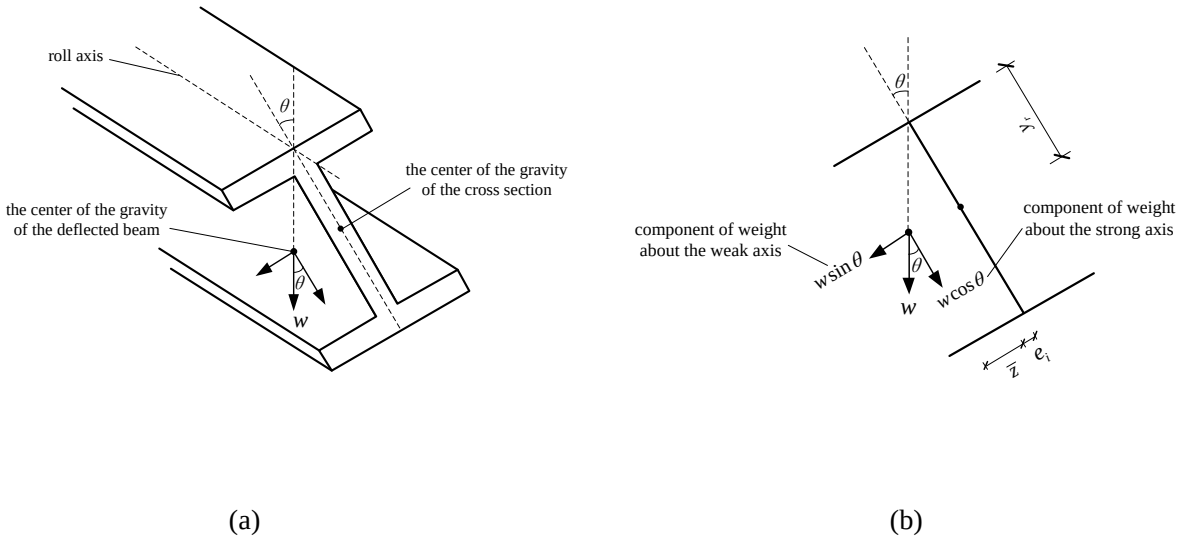

(a) (b)

Figure 2.1 Equilibrium of the beam in tilted position: (a) 3D and (b) frontal views

First of all, a theoretical deflection of the center of gravity of the mass of the beam with the full weight W applied about the weak axis, which is assumed as $\bar{z}_0$, should be computed. Then since the component of the weight which causes the lateral deflection of the beam is $w\sin\theta$, the lateral deflection $\bar{z}$ may be calculated from $\bar{z} = \bar{z}_0 \sin\theta$. The deflection at the mid-span of a beam under uniformly distributed loads can be obtained by the well-known formula as shown in equation 2.1. (PCI design handbook, 1992):

$$\beta_y = \frac{5}{384}\frac{wl^4}{EI_y} \tag{2.1}$$

β_y: The deflection of the weak axis at the mid-span section of the beam

I_y: The minor inertia of the beam

But, $\bar{z}_0$ is defined as the distance to the center of gravity of the deflected arc of the beam, not the maximum deflection calculated in equation 2.1 (Swann, 1971). Therefore, $\bar{z}_0$ may be calculated as approximately $2/3$ of β_y as shown in equation 2.2.

$$\bar{z}_0 = \frac{1}{120}\frac{wl^4}{EI_y} = 0.64\beta_y \tag{2.2}$$

As it is defined before, $\bar{z}_0$ can be only seen as a theoretical deflection of the center of the gravity of the mass of the beam, it is not the final deflection of the weak axis at the mid-span section. Furthermore, most beams would fail when all the weight were applied about the weak axis before reaching the equilibrium state. The smaller quantity which is the final deflection of the beam respect to the weak axis should be calculated from equation 2.3:

$$\bar{z} = \bar{z}_0 \sin\theta \tag{2.3}$$

From Figure 2.1b, an equation regarding the lateral deflection and roll angle can be expressed as equation 2.4.

$$\tan\theta = \frac{\bar{z}_0 \sin\theta + e_i}{y_r} \tag{2.4}$$

For a specific beam, y_r and $\bar{z}_0$ can be obtained from the physical properties of the cross section of the beam and the quantity of the loads. In most cases, θ is sufficiently small (around 0.2 radian or even less) so that the approximation $\theta \approx \sin\theta \approx \tan\theta$ can be used to simplify equation 2.4.

$$\theta = \frac{e_i}{y_r - \bar{z}_0} \tag{2.5}$$

Or it can also be re-written as equation 2.6 (recalling that $\theta_i = \frac{e_i}{y_r}$):

$$\theta = \theta_i\left(\frac{1}{1 - \bar{z}_0/y_r}\right) \tag{2.6}$$

It is observed from equation 2.6 that when $\bar{z}_0$ approaches y_r, the denominator approaches zero and the tilting angle θ become very large. When $\bar{z}_0$ is equal to y_r, the beam is totally unstable even if the initial imperfections can be ignored. Considering that, Mast defined a gross factor of safety against total instability for a near perfect beam by equation 2.7:

$$\text{FS} = \frac{y_r}{\bar{z}_0} \tag{2.7}$$

For stability, the height of the roll center y_r must be larger than $\bar{z}_0$. Mast claimed that those beams with initial imperfections may fail before total instability is reached, as there is a limit on the angle θ that the lateral bending strength of the beam can tolerate. He defined the maximum angle to be θ_{max} and the value of $y_r/\bar{z}_0$ as $(y_r/\bar{z}_0)_{critical}$ when the tilting angle reaches θ_{max}. From equation 2.6, the critical safety factor can be expressed by equation 2.8:

$$\left(\frac{y_r}{\bar{z}_0}\right)_{critical} = \frac{1}{1-\theta_i/\theta_{max}} \tag{2.8}$$

When the tilting angle reaches the maximum value, it would cause the failure of the beam in lateral bending. So that the actual ration of $y_r/\bar{z}_0$ must exceed the critical value. The safety factor can be redefined by equation 2.9:

$$\text{FS} = \frac{y_r/\bar{z}_0}{(y_r/\bar{z}_0)_{critical}} \tag{2.9}$$

Equation 2.9 can be also written as follows:

$$\text{FS} = \frac{y_r}{\bar{z}_0}\left(1-\frac{\theta_i}{\theta_{max}}\right) \tag{2.10}$$

If the initial imperfection is zero, equation 2.10 and equation 2.7 are the same. In Mast's definition, the lateral elastic properties of the beam represented by $\bar{z}_0$ is assumed to be an important parameter of the factor of safety. The effect of θ_i and θ_{max} can be considered to be a modifying effect on the basic stability represented by $y_r/\bar{z}_0$, accounting for the influence of the initial imperfection.

In Mast's work, he also considered the case for stiff laterally beam which $\bar{z}_0$ is sufficiently small but the safety factor may not be as large as calculated in equation 2.10. However, those beams would also fail if the roll angle exceeds a maximum value. In this case, the effect of the initial eccentricity would be the dominant effect. Thus, another expression of the safety factor was defined in terms of the tilting angle as equation 2.11:

$$\text{FS} = \frac{\theta_{max}}{\theta} \tag{2.11}$$

Substituting equation 2.6 for θ:

$$\mathrm{FS} = \frac{\theta_{max}}{\theta_i}\left(1 - \frac{\bar{z}_0}{y_r}\right) \tag{2.12}$$

Although equation 2.12 is very similar to equation 2.10, the main modifier in equation 2.12 is $(1 - \bar{z}_0/y_r)$. The true factor of safety is the lower one between equation 2.10 and equation 2.12.

In Mast's work, he also took into consideration the effect of lifting points' locations. When the lifting points locate in from the end of the beam, the lateral stability of the beam will be improved. On the one hand, the deflection of the beam is reduced by approximately the fourth power of the net span. On the other hand, the weight of the overhanging ends act as a positive effect to the bending of the beam. Anderson (1971) and Imper and Laszlo (1987) gave the results about how the mid-span deflection is influenced by moving the lifting points from the end towards the middle in equation 2.13 and 2.14.

$$\bar{z}_0 = \frac{w}{12EI_{yy}l}\left(\frac{1}{10}l_1^5 - a^2l_1^3 + 3a^4l_1 + \frac{5}{6}a^5\right) \tag{2.13}$$

$$l_1 = l - 2a \tag{2.14}$$

Mast also mentioned that there were other effects should be taken into account when calculating the safety factor. For example, the end blocks normally may be safely (conservatively by 5 to 10 percent) disregarded to the computation of $\bar{z}_0$. It is sufficiently accurate to assume the centroid of the mass is shifted upward by 2/3 of the midspan camber due the combination of self-weight and prestressing force. The effect of inclination angle of the lifting cables was also considered in this study. When the beam is lifted by using inclined cables, the critical buckling load P_{cr} is:

$$\mathrm{P}_{cr} = \frac{\pi^4 EI_y}{l_1^2} \tag{2.15}$$

The quantity $\bar{z}_0$ will be magnified by approximately the quantity $(1 - P/P_{cr})$, where P is the horizontal component of the tension in the inclined cable, multiplied by a factor of safety.

- Mast put forward some recommendations which may increase the lateral stability of the beams hanging from cables in the last part of this paper.The most effective methods of increasing lateral stability of the beam during lifting stage would be moving the lifting point inward from the ends.
- Raising the roll axis, such as providing a yoke attached to the beam at the lifting point or by using a pair of inclined lifting loops, so that y_r is increased which will yield a higher value of the safety factor.
- Increasing the modulus of elasticity *E* so that the stiffness of the beam is increased as well.
- Adding bracing to the beam in order to increase the strength of the beam in lateral bending. Though this method is commonly used in practical, it is also the one with less effectivity.
- Changing the cross section of the beam by enlarging the bottom flange. On the one hand, this can lower the

center of gravity and increase y_r as well as I_{yy}. On the other hand, the bottom flange is under compression and not as subject to loss of stiffness through cracking as is the top flange. However, this method is not practical in a particular project.

Walter L. Peart, Edward J. Rhomberg, Ray W. James

In this paper, the authors mainly discussed about the influence of the camber to the safety of the girder during lifting stage. In the case of prestressed concrete girder, an initial camber can be commonly found due to the prestressing forces. The camber may cause the location of the resultant load to be moved above the torsional center of the beam, which will further produce additional torsional moment and increase the lateral displacement. Based on the differential equations which describe the phenomenon of buckling of the girder due to lateral bending, twisting and warping (Timoshenko and Gere 1961), the authors compared the critical buckling load of the beam considering 3 different types of supports: (1) simply supported; (2) suspended by cables at the ends; (3) suspended by cables located and equal distance from the ends of the member.

The coordinate system was defined as follows (see Figure 2.2 and 2.3). The system coordinate axes *x*, *y* and *z* (Figure 2.2) were fixed at both the vertical and transversal center of the girder and would not be changed along the deformation. The local coordinate axes ξ, ς, η (Figure 2.3) located on different cross sections and would be changed with the deformation. The differential equations describing the bending and torsional behavior of a beam were given by Timoshenko and Gere (1961). Equation 2.16 and Equation 2.17 describe the beam's reaction to bending, while Equation 2.18 accounts for the beam's torsional response.

In this paper, the authors firstly considered the case of uniformly loaded and simply supported beam (see Figure 2.4).The equation for a free body diagram after taking into account the influence of different magnitudes of initial camber was rebuilt by the authors.. Meanwhile, the boundary condition was also applied to the formulas. After solving those equations, relation between two non-dimensional variables with different magnitudes of camber was obtained: q_{cr}/Eb and $l/2h$. q_{cr} represents the critical vertical loads which cause the buckling of the beam. *E* and *l* are the elastic modulus and the length of the beam, respectively. *b* and *h* are the width and height of the cross section of the beam, respectively. It wasconcluded that the simply supported beam behaved almost the same as the one without camber, which meant the critical vertical loads for the beams with different initial camber did not differ much from those of the beam without camber.

$$EI_{\xi}\frac{d^2v}{dz^2} = M_{\xi} \tag{2.16}$$

$$EI_{\eta}\frac{d^2u}{dz^2} = M_{\eta} \tag{2.17}$$

$$C\frac{d\phi}{dz} - C_1\frac{d^3\phi}{dz^3} = M_{\zeta} \tag{2.18}$$

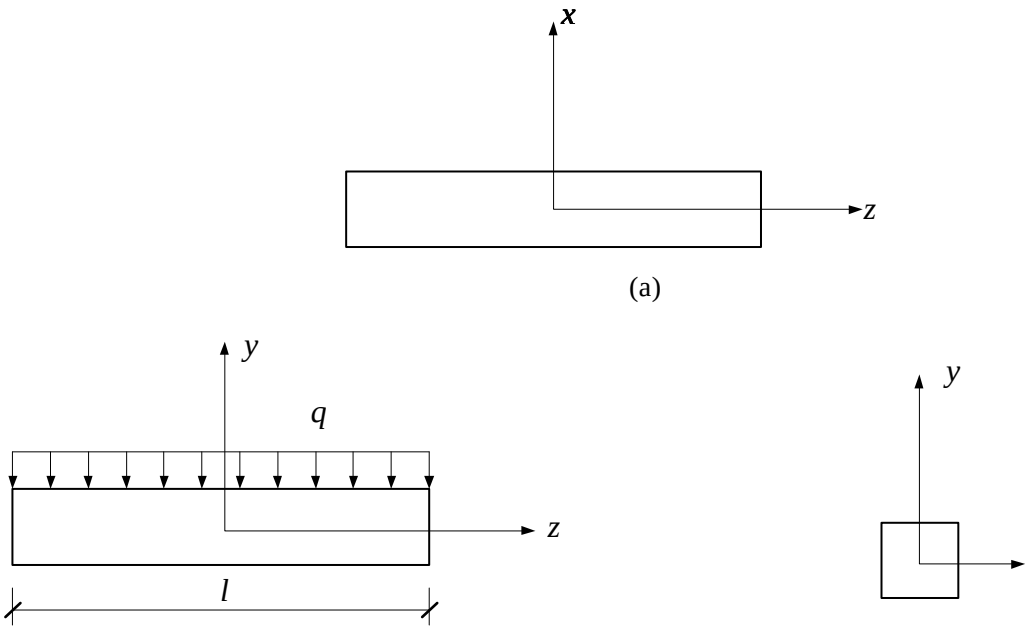

Figure 2.2. Description of the system axes: (a) top, (b) side and frontal views of the girder

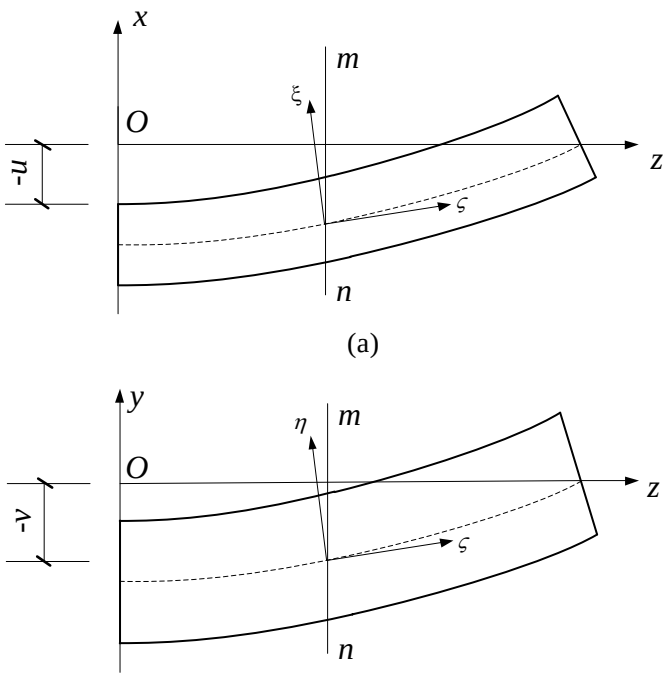

Figure 2.3. Description of the local axes: (a) top; (b) side views of the girder

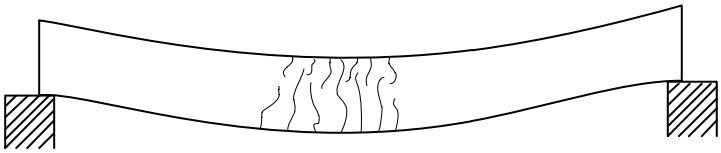

Figure 2.4. Simply supported beam

The second case was the beam suspended at ends (see Figure 2.5). The analysis process was similar to the previous one. The differential equations used for describing the buckling behavior in this case were the same as for the simply supported case. But the boundary conditions were different.Conclusions obtained after applying theses equations to the beams with different ratio of $l/2h$ and different magnitudes of camber were not the same as previous ones. . It was found that when the amount of increase varies with the length of the member, there was a clear indication that camber can play a significant role in determining the critical buckling load for a suspended member.

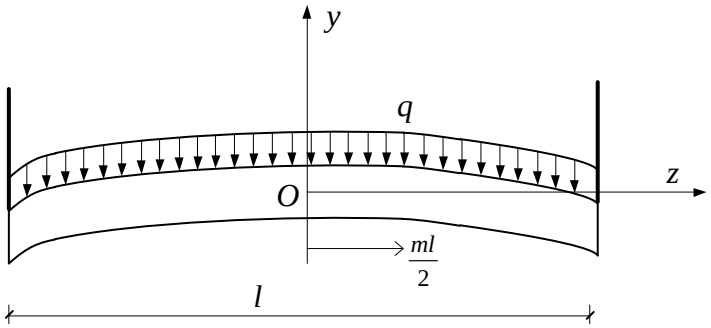

Figure 2.5. Suspended from ends

The third case was the beam suspended at equal distance from ends (see Figure 2.6). The equation derived for the moments was modified because the support conditions were changed. Also, the boundary conditions were different as well. Some continuous conditions at the lifting sections should also be taken into consideration in the analysis. Relations of q_{cr}/Eb against $l/2h$ with or without camber by changing the locations of lifting points were plotted. It was found out that the value of the magnitude and direction of the change of critical buckling load was dependent on the location of the pickup points. The beam with lifting points positioned at the ends of the member (the second case) was the most vulnerable one against buckling. The beam with lifting points located at 1/5l from the ends yielded the maximum critical loads (also larger than that of the simply supported beam), where the positive and negative internal moments of the member balanced. Thus the effects of lifting for members with cross sections that are symmetric about the neutral axis were optimized in this analysis (Peart, Rhomberg and James, 1992). However, this location was not commonly used in practical for many members due to design constraints. Usually, 1/10l was chosen to be the average pickup location from the ends, which the buckling load was higher

than that when the pickup points were at the ends, but lower than that for the simply supported.

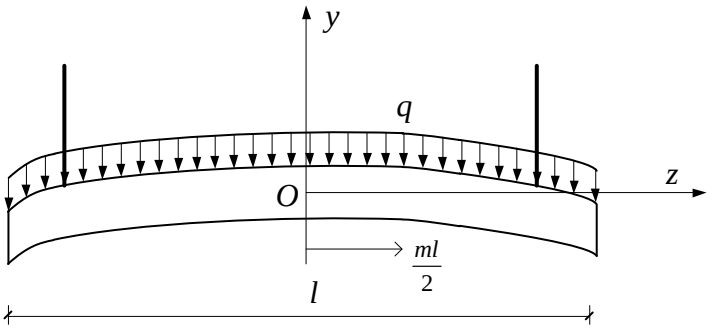

Figure 2.6. Suspended at equal distance from ends

Summarizing, the authors argued that camber reduced the critical buckling load of girders. Therefore, camber cannot be neglected in the design process of prestressed girders while being lifted. The longer the member is, the smaller the critical load which caused buckling would be. The amount of the decrease of critical load was dependent on the magnitude of camber as well as the support type of the member. Simple supports could provide more lateral stability to the beam. Being lifted by loops could decrease or increase the lateral stability of the beam depending on the locations of the loops.

Raymond H. Plaut, Cristopher D. Moen, 2013

Raymond Plaut and Cristopher Moen aimed to build analytical solutions for displacements, forces and moments in a basis curved beam during lifting by two cables. In their paper – *Analysis of Elastic, Doubly Symmetric, Horizontally Curved Beams during Lifting (2013)*, a circularly curved beam that was suspended at two symmetric locations by vertical or inclined cables was analyzed based on the following assumptions:

- The beam is circularly curved (horizontally) with small curvature.
- The cross-sectional dimensions are small compared with the radius of curvature.
- The cross section is uniform and doubly symmetric, and its center of gravity coincides with its shear center.
- The material is homogeneous and linearly elastic.
- Distortion of cross sections in plane is neglected.
- Camber, prestresses, and residual stresses are not included.
- Deformations are small.

The problem is statically determinate and is symmetric about the mid-span of the beam, thus, only the right half of the beam is analyzed (see Figure 2.7). R is the radius of curvature of the unstrained beam, L is the length of the beam, A is the area of the cross section, E is the modulus of elasticity, G is the shear modulus, J is the torsional constant, C_w is the warping constant, and q is the self-weight per unit length. The central angle of the beam is 2α. The cylindrical coordinate θ is zero at the midspan section. The beam is lifted by two cables. D and K are the

lifting points at a distance *a* from ends and a height H above the shear center. The line passing through these two points are the roll axis of the beam. The inclination angle of the lifting cable is ψ and the offset of the center of the beam from the chord through the ends is denoted δ. The geometric relations among these parameters are shown in equation 2.19:

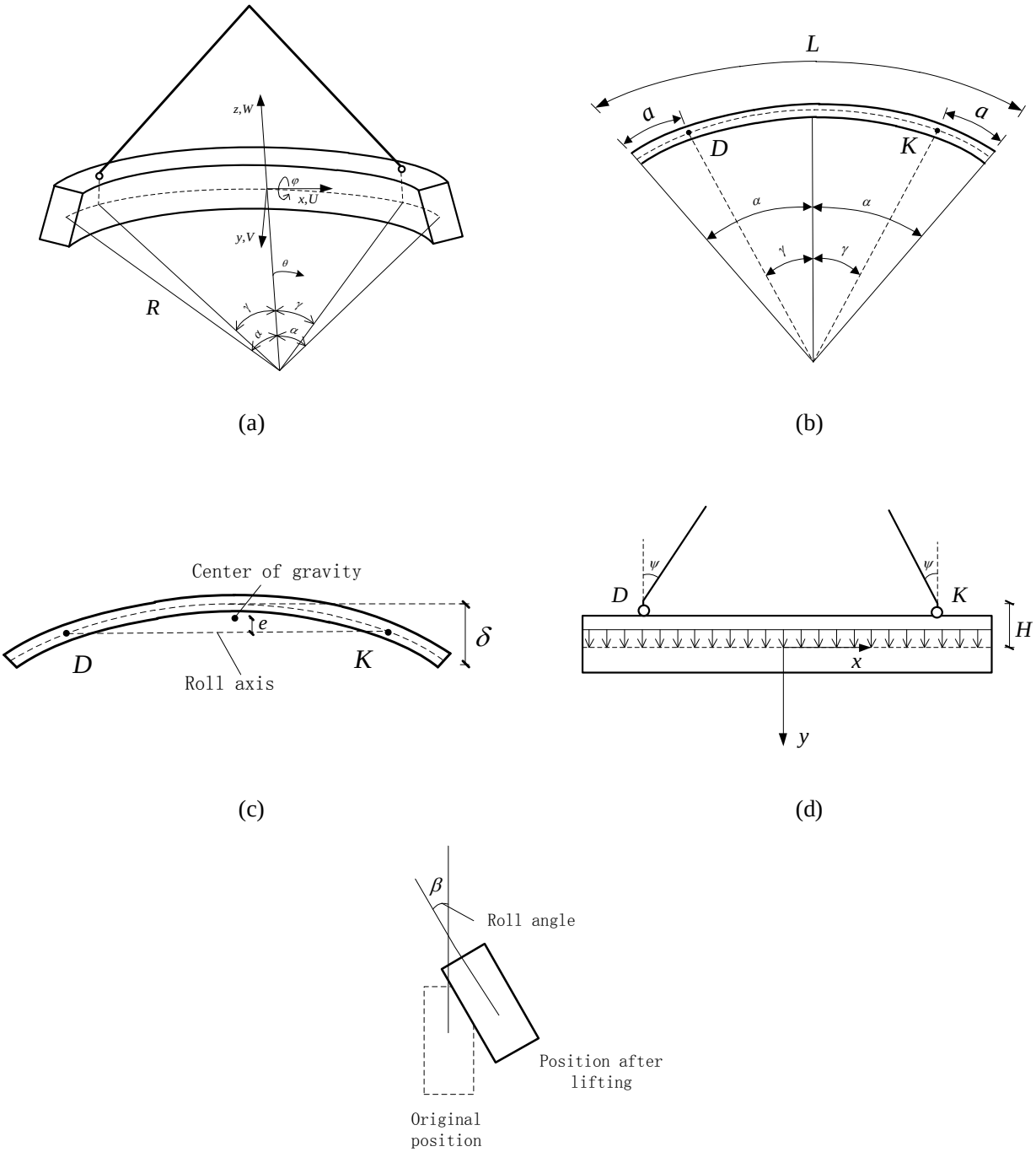

Figure 2.7. Geometry of the curved beam

$$\frac{\delta}{L}=\frac{1-cos\alpha}{2\alpha},\qquad \frac{a}{L}=\frac{\alpha-\gamma}{2\alpha},\qquad \frac{L}{R}=2\alpha,\qquad \frac{e}{R}=\frac{sin\alpha-\alpha cos\gamma}{\alpha} \tag{2.19}$$

When α is very small, approximations can be applied as:

$$\alpha\approx 4\frac{\delta}{L},\qquad \gamma=4\frac{\delta}{L}\left(1-\frac{2\alpha}{L}\right) \tag{2.20}$$

If the center of gravity of the beam does not lie vertically under the roll axis, the beam will tilt about the roll axis till the center of gravity lie in the same vertical plane that includes the roll axis. If the beam is rigid, the roll angle can be found by $\tan\beta_{rigid}=e/H$. When the beam is not rigid, both e and H will be changed due to the self-weight. These variables can be assessed by integral as equation 2.21 and 2.22:

$$e'=\frac{1}{L}\int_{-\frac{L}{2}}^{\frac{L}{2}}(R+W)cos\theta dx-Rcos\gamma \tag{2.21}$$

$$H'=H+\frac{1}{L}\int_{-\frac{L}{2}}^{\frac{L}{2}}Vdx \tag{2.22}$$

where V and W are the strong-axis deflection and weak-axis deflection respectively. V is assumed to be negligible compared with H, then the roll angle β can be expressed by equation 2.23:

$$\mathrm{H}\alpha\tan\beta=(sin\alpha-\alpha cos\gamma)R+z_0\alpha sin\beta \tag{2.23}$$

where z_0 is the lateral deflection of the center of gravity with the self-weight applied laterally (Mast, 1989).

$$z_0=\frac{q\left(0.1{L_1}^5-a^2{L_1}^3+3a^4L_1+1.2a^5\right)(1-\mu)}{12EI_yL} \tag{2.24}$$

With

$$L_1=L-2a,\mu=qL{L_1}^2\frac{tan\psi}{2\pi^2EI_y} \tag{2.25}$$

When the roll angle is relatively small, the roll angle β will be:

$$\beta = \frac{(sin\alpha - \alpha cos\gamma)R}{(H - z_0)\alpha} \tag{2.26}$$

The authors also conducted formulas for calculating the internal forces (see Figure 2.8) and moments along the beam based on the following non-dimensional quantities:

$$\begin{gathered} \mathrm{h} = \frac{H}{L}, n_x = \frac{N_x}{qL}, n_y = \frac{N_y}{qL}, n_z = \frac{N_z}{qL}, m_x = \frac{M_x}{qL^2}, m_y = \frac{M_y}{qL^2}, m_z = \frac{M_z}{qL^2}, u = \frac{U}{L}, \\ v = \frac{V}{L}, w = \frac{W}{L}, \lambda_x = \frac{GJ}{qL^3}, \lambda_y = \frac{EI_y}{qL^3}, \lambda_z = \frac{EI_z}{qL^3}, \lambda_C = \frac{EC_w}{qL^5}, \lambda_A = \frac{EA}{qL} \end{gathered} \tag{2.27}$$

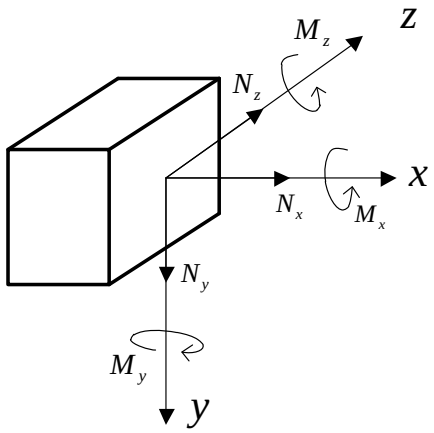

Figure 2.8. Internal forces applied on the cross section along the beam

Equations 2.28-31 below are valid for both uniform torsion and non-uniform torsion cases.

For $0 \leq \theta < \gamma$,

The axial internal forces are:

$$\begin{gathered} n_x = \frac{1}{2\alpha}(\theta sin\theta sin\beta - \alpha cos\theta tan\psi) \\ n_y = -\frac{1}{2\alpha}\theta cos\beta \\ n_z = -\frac{1}{2\alpha}(\theta cos\theta sin\beta + \alpha sin\beta tan\psi) \end{gathered} \tag{2.28}$$

The internal moments are:

$$\begin{gathered} m_x = \frac{1}{4\alpha^2}(c_1 sin\theta - \theta cos\beta), \\ m_y = \frac{1}{4\alpha^2}(cos\alpha + \alpha sin\gamma - cos\theta - \theta sin\theta)sin\beta + \frac{1}{4\alpha}(cos\theta - cos\gamma)tan\psi, \end{gathered} \tag{2.29}$$

$$m_z = \frac{1}{4\alpha^2}(cos\beta - c_1 cos\theta)$$

where c_1 can be found in (Plaut and Moen, 2013), along with $c_2, c_3, \cdots, c_{29}$.

For $\gamma < \theta \leq \alpha$, the internal forces are:

$$\begin{aligned} n_x &= \frac{1}{2\alpha}(\theta - \alpha) sin\theta sin\beta, \\ n_y &= \frac{1}{2\alpha}(\alpha - \theta) cos\beta, \\ n_z &= \frac{1}{2\alpha}(\alpha - \theta) cos\theta sin\beta \end{aligned} \tag{2.30}$$

The internal moments are:

$$\begin{aligned} m_x &= \frac{1}{4\alpha^2}[\alpha - \theta - sin(\alpha - \theta)] cos\beta \\ m_y &= \frac{1}{4\alpha^2}[cos\alpha - cos\theta + (\alpha - \theta) sin\theta] sin\beta \\ m_z &= \frac{1}{4\alpha^2}[1 - cos(\alpha - \theta)] cos\beta \end{aligned} \tag{2.31}$$

The weak-axis bending deflection $w(\theta)$ is (valid for both uniform torsion and non-uniform torsion):

$$w = \frac{1}{64\alpha^4\lambda_y}\{[-4c_2 + 3\theta sin\theta + (c_3 - \theta^2) cos\theta] sin\beta + (4\alpha cos\gamma - 2\alpha\theta sin\theta + c_4 cos\theta) tan\psi\} \tag{2.32}$$

$$(0 \leq \theta \leq \gamma)$$

$$w = \frac{1}{64\alpha^4\lambda_y}\{[4(cos\theta sec\gamma - 1) cos\alpha + (c_5 + 3\theta) sin\theta + (\gamma - \theta)(c_6 + \theta) cos\theta - c_7 cos\theta] sin\beta + c_8 sin(\gamma - \theta) tan\psi\} \tag{2.33}$$

$$(\gamma \leq \theta \leq \alpha)$$

Strong-axis bending and twist angle for uniform torsion:

Twist angle

$$\begin{aligned} \phi &= \frac{(\lambda_x + \lambda_z)}{16\alpha^3\lambda_x\lambda_z}(-2cos\beta + c_{13} cos\theta + c_1\theta sin\theta) \quad (0 \leq \theta \leq \gamma) \\ \phi &= \frac{1}{64\alpha^3\lambda_x\lambda_z}(c_{14} + c_{15} sin\theta + c_{16} cos\theta + c_{17}\theta sin\theta + c_{18}\theta cos\theta) \quad (\gamma \leq \theta \leq \alpha) \end{aligned} \tag{2.34}$$

Deflection

(2.35)

$$v = \frac{1}{32\alpha^4\lambda_x\lambda_z}(c_{19} - \lambda_z\theta^2 cos\beta + c_{20}cos\theta + c_{21}\theta sin\theta) \quad (0 \le \theta \le \gamma)$$

$$v = \frac{1}{64\alpha^4\lambda_x\lambda_z}(c_{22} + 2\alpha c_{23}\theta - c_{23}\theta^2 + c_{24}sin\theta + c_{25}cos\theta + c_{26}\theta sin\theta + c_{27}\theta cos\theta)$$
$$(\gamma \le \theta \le \alpha)$$

Strong-axis bending and twist angle for non-uniform torsion:

Twist angle

$$\begin{gathered}\phi = a_1 sin\theta + a_2 cos\theta + a_3 sinh(k\theta) + a_4 cosh(k\theta) + c_{28} + c_1 c_{29}\theta sin\theta \quad (0 \le \theta \le \gamma) \\ \phi = b_1 sin\theta + b_2 cos\theta + b_3 sinh(k\theta) + b_4 cosh(k\theta) + c_{28} - c_{29}\theta sin(\alpha - \theta)cos\beta \\ (\gamma \le \theta \le \alpha)\end{gathered} \tag{2.36}$$

where $k = \sqrt{\lambda_x/(4\alpha^2\lambda_C)}$

Deflection

$$\begin{aligned}v = \frac{1}{32\alpha^4k^2\lambda_z}\{&e_1 + e_2\theta + k^2\theta^2 cos\beta + 8k^2\alpha^3\lambda_z c_{28}\theta^2 + 2k^2[c_1 - 8\alpha^3(a_2 + 2c_1c_{29})\lambda_z]cos\theta \\ &+ 16\alpha^3\lambda_z[a_3 sinh(k\theta) + a_4 cosh(k\theta) - k^2(a_1 + c_1c_{29}\theta)sin\theta]\} \\ &(0 \le \theta \le \gamma)\end{aligned} \tag{2.37}$$

$$\begin{aligned}v = \frac{1}{32\alpha^4k^2\lambda_z c_1}\{&e_3 + e_4\theta + 2k^2(c_1 - 16\alpha^3c_1c_{29}\lambda_z)cos(\alpha - \theta)cos\beta \\ &+ k^2c_1(\theta^2 cos\beta + 8\alpha^3c_{28}\lambda_z\theta^2 - 16\alpha^3b_2\lambda_z cos\theta + 16\alpha^3\lambda_z) \\ &\times [b_3c_1 sinh(k\theta) + b_4c_1 cosh(k\theta) - b_1c_1k^2 sin\theta + k^2c_1c_{29}\theta sin(\alpha - \theta)cos\beta]\} \\ &(\gamma \le \theta \le \alpha)\end{aligned}$$

The authors provided an overall method to study the response (internal forces, moments, deflections and rotation angles) of the curved beam lifted by two cables. Most of these can be applied both for uniform and non-uniform torsion. The authors also mentioned that the locations of the lift points play an important role in determining the roll angle and deformations of the beam. For instance, if the lift points locate at around 1/5L inwards from ends of the beam, the roll angle and twist angle would be very small. This was also proved in Peart's work as shown previously. However, due to the constraints of cracking, this location of lifting loops is not practical in construction. The work was also extended based on Yegian (1956) when horizontal eccentricity of the lift points was considered. Lateral wind loads were not taken into consideration in this research work like in Stratford and Burgoyne (2000) since the authors believed that usually lifting would be performed when wind loads were not significant. At last, they emphasized the importance of predicting the behavior of the beam during construction. The main reason was that the maximum stresses and deformations for a curved beam may occur during lifting phase. Even though real beams may not satisfy all the assumptions of this problem analyzed in this paper, the derived equations should be useful in most cases.

Other previous researches which are related to the study in this thesis are summarized in Table 1.1 as follows.

Table 1.1. Researches on lateral stability of girders under transient phases

Year	Type	Main considerations	Outcomes	Authors
1962	Analytical study	-torsional -boundary conditions -lifting positions	A model for calculating the critical vertical loads for precast members during handling and placing	Muller
1987	Analytical study	-lifting positions -plant handling -field handling	Different safety factors for different handling phases were defined. Practical ways of enabling the stability of girders by using external materials were proposed.	Laszlo and Imper
1989	Analytical study with physical model	-initial sweep -camber -lifting positions	A model for evaluating the lateral stability in terms of the safety factor.	Mast
1992	Analytical study with differential equations	- precamber - support types	The influence of precamber to the buckling load of girder with flexible supports	Peart
2000	Analytical study with both finite model and analytical model	- inclined or vertical cables - inclined or vertical lifting yokes - lateral loads - initial imperfections	Methods for predetermining the buckling load, the buckling mode, the load-deflection path of imperfect beams	Stratford and Burgoyne

2.2.2 Summary of different standards and codes regarding lateral instability

Eurocode 2

In section 5.9, it points out that the lateral instability of slender beams should be taken into consideration when it is necessary. For instance, when precast beams are transported or erected at sites, or when there are no sufficient lateral bracing for the beam in finished structure etc. The second order effect regarding lateral instability could be ignored if the following conditions are satisfied:

- for persistent situations: $\frac{l_0}{b} \leq \frac{50}{\left(\frac{h}{b}\right)^{\frac{1}{3}}}$ and $h/b \leq 2.5$
- for transient situations: $\frac{l_0}{b} \leq \frac{70}{\left(\frac{h}{b}\right)^{\frac{1}{3}}}$ and $h/b \leq 3.5$

where:

l_0: the distance between torsional restraints

h: the total depth of the beam in the center of l_0

b: the width of compression flange

PCI – Recommended Practice for Lateral Stability of Precast, Prestressed Concrete Bridge Girders

In this report, it defines the factor of safety which is considered to be a key concept in ensuring the lateral stability of a girder. The factor consists of two parts: the resisting moment M_r and the acting moment M_a (see Figure 2.9).

These can be expressed as:

$$M_r = w\sin\theta \cdot y_r \tag{2.38}$$

$$M_a = w\cos\theta \cdot (\bar{z} + e_i) = w\cos\theta \cdot (\bar{z_0}\sin\theta + e_i) \tag{2.39}$$

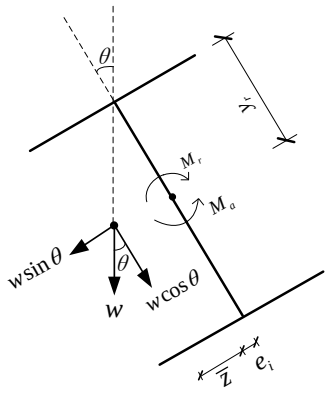

Figure 2.9. Resisting moment and acting moment

The factor of safety is the ratio of M_r to M_a, which to some extent represents the ability of the girder in resisting the acting moment which cause the girder to tilt.

$$\text{FS} = \frac{M_r}{M_a} = \frac{y_r\theta}{\bar{z_0}\theta + e_i} \tag{2.40}$$

The cracking state is defined as the first crack appears on the girder. The roll angle of the girder at this state would

be seen as the maximum roll angle θ_{max} against cracking. Then, the factor of safety against cracking is defined in equation 2.41. Tt is recommended to be at least 1.0, which means the resisting moment is larger than the applying moment at this stage. To put it into another way, the resisting moment is large enough to prevent more tilt, thus the cracks will not appear on the girder.

$$\mathrm{FS} = \frac{M_r}{M_a} = \frac{y_r \theta_{max}}{\bar{z_0}\theta_{max} + e_i} \geq 1.0 \tag{2.41}$$

After the beam starting to crack, the lateral stiffness of the girder would be reduced, so the deflection would be larger under the same load. The effective stiffness after cracking is defined by Mast (1993) as:

$$E_c I_{eff} = \frac{E_c I_g}{(1 + 2.5\theta)} \tag{2.42}$$

Thus the factor of safety becomes:

$$FS = \frac{M_r}{M_a} = \frac{y_r \theta}{z_0 \theta (1 + 2.5\theta) + e_i} \tag{2.43}$$

Unlike the factor of safety against cracking, it recommends that the factor of safety against failure must be larger than 1.5:

$$FS' = \frac{M_r}{M_a} = \frac{y_r \theta'_{max}}{z_0 \theta'_{max}(1 + 2.5\theta'_{max}) + e_i} \geq 1.5 \tag{2.44}$$

What is more, the maximum roll angle can be found by:

$$\theta'_{max} = \sqrt{\frac{e_i}{2.5 z_0}} \tag{2.45}$$

Chinese codes

1. Code for Design of highway Reinforced Concrete and Prestressed Concrete Bridges and Culverts (JTG D62-2004)

In this code, there are no specific provisions for preventing lateral collapse of precast prestressed beam while being lifted. But some construction requirements for beams are proposed in provision 9.3. Some of them are listed as follows.

"*9.3.1 The span of simply supported precast prestressed concrete beam with T section or I section should not exceed 50m.*"

"*Diaphragms should be set at both the middle and the end of one span along the beam with T section or I section.*"

"*The depth of upper flange of T section should not be smaller than 100mm.*"

2. Technical Specifications for Highway Bridges and Culverts (JTJ041-2000)

In section 15, some guidelines are proposed for the construction of assembly beams. These guidelines are suitable for the beams being precasted, transported, stacked and assembled regarding the strength of material, the size of members and etc.

"*15.6.1.2 The strength of the concrete of the beam should not be lower than 75% of the design strength for lifting while it being transported, stacked and lifted.*"

"*15.6.1.10 The technical requirements for lifting tools should be accordance with the regulations of hoisting equipment. The stability of the simply supported precast prestressed beam should be verified if the span exceeds 25m.*"

fib Model Code for Concrete Structures 2010

In this code, life cycle management is considered to be an overall strategy to be used in managing a structure through its development and service life. With the aim of improving its efficiency from a business/engineering point of view, associated performance requirements defined at design stage and all the service life of the structure should be satisfied. In section 3.5, it mentions that in order to develop the structural concept, the lifting capacity at the site should be taken into consideration. However, there is no specific regulation for ensuring the lateral stability of beams under transient phases.

The recommendations for preventing lateral stability failure in current standards are summarized in Table 1.2.

2.2.3 Limitation of current methods

Although the lateral instability problem was analyzed by different researchers with different methods, there are limitations in practical use.

In Mast's (1989) research, he defined the factor of safety against lateral instability. This formula has its physical meaning – that is the resisting moment provided by the section should be larger than the applying moment in order to provide sufficient resistance. He pointed out there is a critical factor which would cause failure in lateral bending when the roll angle θ reaches the maximum angle θ_{max}. Thus, the factor of safety should be larger than this critical value. However, he did not give the method on how to determine the maximum angle. Moreover, Mast discussed in his paper that the camber would affect the lateral stability of the beam because it would shift the center of gravity of the beam upward by 2/3 of the midspan camber. Nevertheless, the value 2/3 of the midspan camber is not precise enough.

In Peart's method, it analyzed the influence of the camber to the stability. Meanwhile, he also compared the effects to the stability of beam under different support conditions. Considering the practical use, he found out the optimal lifting loops' locations which could provide the most stability to the beam among different support conditions. However, Peart did not quantify the influence of the camber in this problem.

Table 1.2. Recommendations for preventing lateral stability failure in current standards

Code or guideline	Recomendation
EN 15050:2008	$e_i \leq \frac{l}{500}$
Eurocode 2*	$\frac{l}{b} \leq \frac{70}{(h/b)^{\frac{1}{3}}}$
	$\frac{h}{b} \leq 3.5$
fib Model Code 2010*	$\frac{l}{b} \leq \frac{50}{(h/b)^{\frac{1}{3}}}$
ACI 318-08*	$\frac{l}{b} \leq 50$
PCI 2016	$FS_{cr} \geq 1.00$
ABNT NBR 6118	$\frac{h}{b} \leq 2.5$
	$\frac{l}{b} \leq 50$
BS:8110-1	$\frac{lh}{b^2} \leq 250$
	$\frac{l}{b} \leq 60$
JTG D62-2004	$l \leq 50$
Spanish Code EHE-08 (Annex 11)	$e_i \leq \frac{l}{750}$

In Plaut's research, though he gave the full formulas to calculate the internal forces and moments as well as the response of the beam while being lifted, those formulas are too complicated to be applied in practical. The design work will not be as efficient as expected.

Regarding the current codes or standards, most of them emphasize that the lateral stability should be taken into consideration while the beam under transient situation, but the further considerations are not given. PCI gives a method to verify the safety condition by using a factor of safety. However, in real cases there are accidents happened even though the conditions are satisfied the regulations. Other standards provide the limitations in terms of sweep or ratio of the section's width to length of girder, which are found to be insufficient reliable in those failure accident. It is apparently these recommendations lack sufficient guidance on preventing stability failure of precast prestressed concrete girders during transient phases.

CHAPTER 3.

PARAMETRIC STUDY OF A HANGING GIRDER

3.1 PROBLEM DEFINITION

The model used in this research program is mainly based on Mast's model. The lateral stability of the precast prestressed concrete girder while being lifted is studied in terms of the factor of safety defined by PCI. The basic assumptions in this research are the same as in Mast's study: (1) the girder is rigidly restrained from rotation at the supports and (2) buckling is caused by the middle part of the span twisting relative to the support.

The problem is depicted in Figure 3.1. The girder is lifted by two cables located at an equal distance a from both ends and a height h_{lift} from the top of the girder. The inclined angle of the cable is ϕ. These three parameters a, h_{lift} and ϕ can be pre-determined by the designer. I-type cross-section girder is established in the scope of this research since its physical properties are more representative. The properties of other types of section can be simplified from this I-section such as T-section or transferred to I-type such as box section. The general geometry of the section is shown in Figure 3.2.

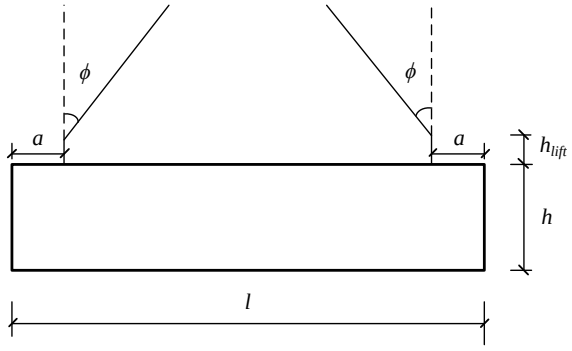

Figure 3.1. Problem definition

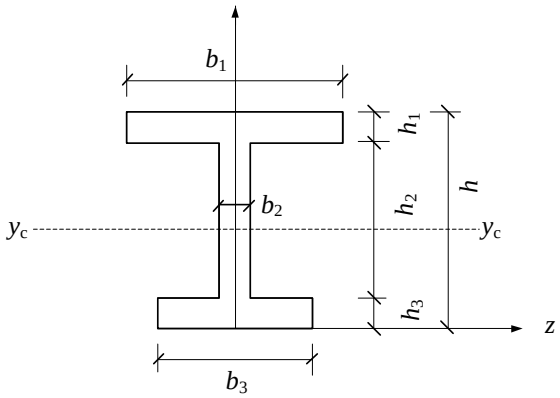

Figure 3.2. Geometry of the cross section

Thus, the general physical properties of the section are listed as follows.

Area:

$$A_c = b_1h_1 + b_2h_2 + b_3h_3 \tag{3.1}$$

Vertical coordinate of the neutral axis:

$$y_{cg} = \frac{h_1b_1\left(h_2 + h_3 + \frac{h_1}{2}\right) + h_2b_2\left(h_3 + \frac{h_2}{2}\right) + h_3b_3\frac{h_3}{2}}{h_1b_1 + h_2b_2 + h_3b_3} \tag{3.2}$$

Major inertia:

$$I_{zz} = \frac{1}{12}b_1{h_1}^3 + b_1h_1(h - y_{cg})^2 + \frac{1}{12}b_2{h_2}^3 + b_2h_2\left(h_3 + \frac{h_2}{2} - y_{cg}\right)^2 + \frac{1}{12}b_3{h_3}^3 + b_3h_3\left(y_{cg} - \frac{h_3}{2}\right)^2 \tag{3.3}$$

Minor inertia:

$$I_{yy} = \frac{1}{12} h_1 {b_1}^3 + \frac{1}{12} h_2 {b_2}^3 + \frac{1}{12} h_3 {b_3}^3 \tag{3.4}$$

3.2 MECHANISM OF THE MODEL

The mechanism of the model is similar to that in Mast's model. Since the torsional deformation is neglected, the problem can be transferred into simple lateral bending and equilibrium problem. When the girder is not perfectly fabricated, where the center of gravity is not at the same vertical plane which includes the roll axis passing through the two lifting points, the girder is prone to tip around the roll axis (see Figure 3.3). Then the self-weight of the girder will be decomposed in two directions at the midspan section – perpendicular and parallel to the neutral axis $y_c - y_c$ (see Figure 3.4). The lateral deflection of the girder will be increased under the component of the self-weight $q\sin\theta$, which will further result in the shift of the center of gravity and cause an extra roll angle θ of the girder. In turn, the self-weight components will increase as well and make the girder deflect more. The equilibrium state of the girder will be reached when the center of gravity stays in the same vertical plane includes the roll axis. Or the girder can also collapse before reaching this equilibrium state.

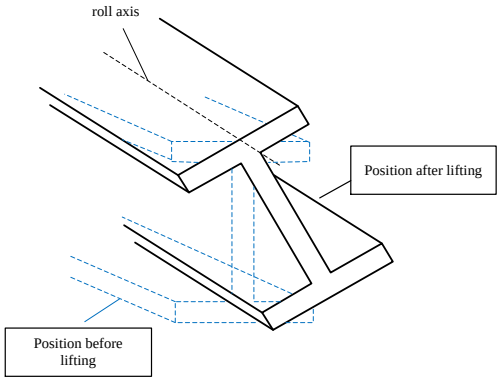

Figure 3.3. The initial tilt of the girder when lifting

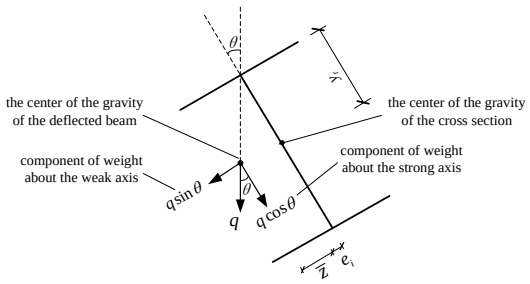

Figure 3.4. The midspan cross section of the tilt girder and the components of self-weight applied on the section

During this iterative-equilibrium process, the girder deforms and the internal stresses increase. If the stress at some points reaches the tensile strength of the concrete (f_{ct}), the girder cracks and the stiffness of the girder decreases, which will cause larger deflection of the girder. According the experimental and numerical results obtained by Mast (1993), the effective stiffness of the cracked girder can be assessed by dividing the stiffness by the amount $(1 + 2.5\theta)$ (see equation 2.42). Thus, the first cracking point can be seen as the critical point to be controlled during this process. If the factor of safety fulfills the regulation in PCI at the cracking section, the girder can be seen as safe during lifting.

3.3 CRACKING OF THE GIRDER DURING LIFTING

The forces applied on the cross section include the self-weight, prestress of the reinforced bars, and the forces in the lifting cables (see Figure 3.5). For this particular cross-section, the maximum tensile stress is expected to occur at the left corner of the upper flange of the cross section at the midspan of the girder.

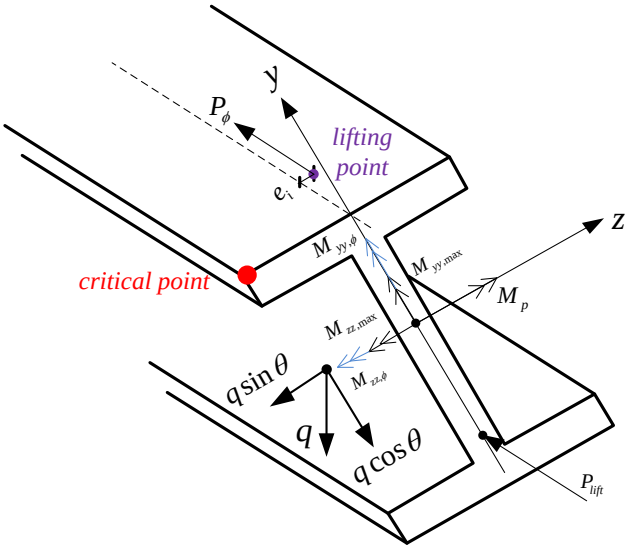

Figure 3.5. Forces and moments applied on the cross section

The forces and moments applied on the midspan section are defined as follows:

P_{lift}: Longitudinal compressive force caused by the prestress, considering the prestress losses before lifting. If the initial prestress of the reinforced bar is P_0, the value of P_{lift} will be $P_{lift} = (1 - \Psi)P_0$, where Ψ is the prestress losses factor. A value of Ψ = 0.15 has been considered as suitable in this research.

P_φ: Longitudinal compressive force caused by the horizontal component of the force in the lifting cable.

M_p: The moment applied about the major axis caused by the prestress, $M_p = P_{lift}e_p$, where e_p is the eccentricity of the prestress reinforced bar to the center of gravity.

$M_{zz,max}$: The moment applied about the major axis caused by the component of the self-weight qcosθ, $M_{zz,max} = \frac{qcos\theta {l_a}^2}{8}$, where l_a is the distance between the lifting points, $l_a = l - 2a$. The part of the girder between those two lifting points can be seen as a simply support girder. The favorable effect of the part from the lifting point to the end is neglected in the analysis.

$M_{yy,max}$: The moment applied about the minor axis caused by the component of the self-weight qsinθ. $M_{yy,max} = \frac{qsin\theta {l_a}^2}{8}$.

$M_{zz,\varphi}$: The moment applied about the major axis caused by the horizontal component force in the lifting cables. $M_{zz,\varphi} = P_\varphi\left(h + h_{lift} - y_{cg} - \delta_G\right)$. δ_G is the precamber of the girder caused by prestress.

$M_{yy,\varphi}$: The moment applied on the minor axis caused by the horizontal component force in the lifting cables. $M_{yy,\varphi} = P_\varphi e_i$. $\bar{z_0}$ is the deflection of the center of gravity with the full weight applied about the minor axis.

The tensile stress at the left corner of the upper flange at the midspan section is:

$$\sigma_t = \frac{-\left(P_{lift} + P_\varphi\right)}{A_c} + \frac{M_p\left(h - y_{cg}\right)}{I_{zz}} - \frac{\left(M_{zz,\max} + M_{zz,\varphi}\right)\left(h - y_{cg}\right)}{I_{zz}} + \frac{\left(M_{yy,max} + M_{yy,\varphi}\right)\left(\frac{b_1}{2}\right)}{I_{yy}} \tag{3.5}$$

When σ_t reaches the maximum tensile strength f_{ctm} of the concrete, the concrete will start to crack.

$$f_{ctm} = 0.3{f_{ck}}^{2/3} \tag{3.6}$$

where f_{ck} is the characteristic value of the compressive strength of the concrete.

The critical condition can be shown as equation 3.7.

$$\sigma_t = f_{ctm} \tag{3.7}$$

From equation 3.5, it is known that all the parameters can be determined by the physical properties of the section or the properties of the material except the roll angle θ. Thus, the roll angle at cracking state θ_{cr} can be found by solving equation 3.7. For most applications, θ is sufficiently small (say 0.2 radian or less), so that the approximation $\theta \approx \sin\theta \approx \tan\theta$ and $\cos\theta \approx 1$ may be used (Mast, 1989). Hence, some equations can be simplified as equation 3.8 and 3.9. Then θ_{cr} can be calculated by equation 3.10.

$$M_{yy,max} = \frac{qsin\theta {l_a}^2}{8} \approx \frac{q\theta {l_a}^2}{8} \tag{3.8}$$

$$M_{zz,max} = \frac{qcos\theta {l_a}^2}{8} \approx \frac{q {l_a}^2}{8} \tag{3.9}$$

$$\theta_{cr} = \left[f_{ctm} + \frac{P_{lift} + P_{\varphi}}{A_c} - \frac{M_p(h - y_{cg})}{I_{zz}} + \frac{(M_{zz,max} + M_{zz,\varphi})(h - y_{cg})}{I_{zz}} - \frac{M_{yy,\varphi} b_1}{2I_{yy}} \right] \times \frac{16 I_{yy}}{b_1 q {l_a}^2} \quad (3.10)$$

Once the roll angle θ_{cr} at cracking state is obtained, the factor of safety can be calculated by equation 3.11 and it is recommended in the PCI handbook that this factor should be at least 1.0.

$$\mathrm{FS}_{cr} = \frac{M_r}{M_a} = \frac{y_r \theta_{cr}}{\bar{z_0} \theta_{cr} + e_i} \geq 1.0 \quad (3.11)$$

y_r is the distance between the center of gravity and the lift point, considering the precamber δ_G which shifts upward the center of gravity.

$$y_r = h + h_{lift} - y_{cg} - \delta_G \quad (3.12)$$

$\bar{}$ is the midspan deflection with the full weight applied about the weak axis (see equation 3.13). Anderson (1971) and Imper and Laszlo (1987) have taken into consideration the location of the lifting points which are moved in from the end at a distance a. Mast argued in his work that locating the lifting point even a small distance in from the end can dramatically improve the lateral bending stability. It is not only because the deflection reduced by approximately the fourth power of the net span, but also because of the favorable effect of the overhanging ends which will decrease the midspan deflection of the girder.

$$\bar{z_0} = \frac{q}{12 E I_{yy} l} \left(\frac{1}{10} l_a^5 - a^2 l_a^3 + 3a^4 l_a + \frac{5}{6} a^5 \right) \quad (3.13)$$

e_i is the transversal distance from the roll axis to the center of gravity of the girder considering the initial eccentricity e_0 of the loops and lateral imperfection f (measured or allowed) expressed as a fraction of the total length of the girder (see equation 3.14). This lateral imperfection can be due to non-uniform solar radiation, lateral eccentricity of the prestress, imperfections of the molds etc.

$$e_i = e_0 + \frac{2}{3} f \quad (3.14)$$

All the parameters of the material and the section above can be determined in advance. With the help of Matlab, it is easy to obtain the factor of safety FS_{cr} under different combinations of sections and materials. In the following part, case studies are carried out with different parameters.

3.4 PARAMETRIC STUDY

3.4.1 Introduction

According the aspects gathered in Chapter 3 regarding the lateral stability, the critical state of the girder being lifted to be controlled is the cracking state. Once this state is determined, the factor of safety can be found and those with value larger than 1.0 can be seen as acceptable, which means the girder is safety during lifting process.

However, the safety of factor is dependent on many parameters such as the length of the girder, the area of the cross-section, the location of the lifting loops, the concrete strength etc. The control variable method is used in order to determine the relations of the factor of safety between different parameters.

3.4.2 Geometry

Four main sections are chosen from a catalog, namely I140B120, I160B120, I180B120, I200B120. The shapes of the upper flanges and lower flanges are the same in these 4 sections. The heights of the web are increased by 0.20m each from 1.40m to 2.00m. The section is shown in Figure 3.6.

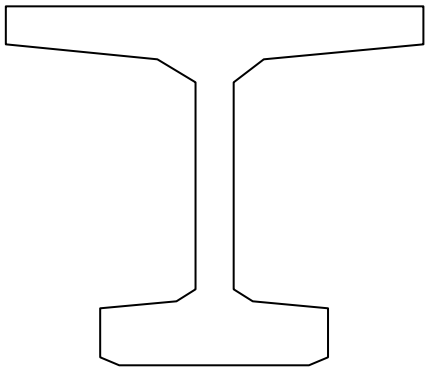

Figure 3.6. Shape of the cross section

The geometric characteristics of the sections are listed in Table 3.1.

Table 3.1. Geometric characteristics of the cross section

Section Type	$b_1(m)$	h(m)	$A_c(m^2)$	$I_{zz}(m^4)$	$I_{yy}(m^4)$
I140B120	1.20	1.40	0.4927	0.1341	0.0204
I160B120	1.20	1.60	0.5230	0.1872	0.0204
I180B120	1.20	1.80	0.5530	0.2507	0.0205
I200B120	1.20	2.00	0.5833	0.3252	0.0206

- The lengths of the girder are: 20, 30, 40, 50 and 60 m.
- The characteristic compressive strengths of the concrete are: 30 MPa (C30), 40 MPa (C40), 50 MPa (C50), 60 MPa (C60).
- The longitudinal distances a of the lifting loops from the end of the girder are: 0, $l/10$, $l/5$.
- The lateral imperfections f are: $l/500$, $l/750$

3.4.3 Prestressing force

Applying prestress on concrete structure aims to offset part or full of the tensile stress, thus the deformation and damage of the structure can be reduced during service life. In precast prestressed concrete girder, the deflection of the girder can be reduced due to the precamber caused by the prestress. The number and width of cracks will also be reduced due to the compressive force applied on the structure. Though prestress has many benefits for the behavior of the girder, over magnitudes of prestress could result in unnecessary damage to the structure. In this particular research, the basic principle for determining the magnitude of prestress is to prevent cracks appearing on the girder before lifting. Before lifting, only the prestress force and self-weight are applied on the girder. For a simply support girder, the maximum bending moment caused by the self-weight occurs at the midspan section whilst the maximum prestress force applies on the end section. Therefore, these two sections are the critical sections to be controlled before lifting.

Midspan section

The maximum tensile stresses appear at the upper flange (upper layer). It has to be lower than the maximum tensile stress of the concrete f_{ctm} in order to prevent cracks before lifting.

$$\sigma_{tmax,upper}^{mid} = -\frac{P_0}{A_c} + \frac{P_0 e_p}{I_{zz}}(h - y_{cg}) - \frac{M_G}{I_{zz}}(h - y_{cg}) \leq f_{ctm} \tag{3.16}$$

The maximum compressive stress will appear at the bottom of the section. As it recommends in 5.10 section of Eurocode 2, the concrete compressive stress in the structure resulting from the prestressing force and other loads acting at the time of tensioning or release of prestress, should be limited to:

$$\sigma_{cmax,lower}^{mid} = -\frac{P_0}{A_c} - \frac{P_0 e_p}{I_{zz}} y_{cg} + \frac{M_G}{I_{zz}} y_{cg} \geq -0.6 f_{ck} \tag{3.17}$$

End section

The maximum tensile stress will appear at the top of the section. Like on the midspan section, it has also to be lower than the maximum tensile stress of the concrete f_{ctm}.

$$\sigma_{tmax,upper}^{end} = -\frac{P_0}{A_c} + \frac{P_0 e_p}{I_{zz}}(h - y_{cg}) \leq f_{ctm} \tag{3.18}$$

Like on the midspan section, the maximum compressive stress resulting from prestressing force should be limited to:

$$\sigma_{cmax,lower}^{mid} = -\frac{P_0}{A_c} - \frac{P_0 e_p}{I_{zz}} y_{cg} \geq -0.6 f_{ck} \tag{3.19}$$

From all the equations above, it can be seen that there is a maximum value of prestressing force for each type of section with a particular concrete strength. The critical prestressing force can be obtained from equation 3.18, which can be expressed as equation 3.20:

$$P_0 = \frac{f_{ctm}}{\left[\frac{e_p(h-y_{cg})}{I_{zz}} - \frac{1}{A_c}\right]} \tag{3.20}$$

The predefined maximum initial prestressing forces used for different cross sections with different concrete strength are listed in Table 3.2 as follows.

Table 3.2. Maximum initial prestressing forces applied on the girders with different cross sections

Section Type	P_0(kN)			
	C30	C40	C50	C60
I140B120	2774	3360	3899	4403
I160B120	2812	3406	3953	4464
I180B120	2837	3437	3988	4504
I200B120	2853	3456	4010	4529

As it explains in the problem definition, a reduction factor Ψ with a value of 0.15 is used in order to consider the prestress loss during lifting. Thus, the prestressing force applied on the girder during lifting is summarized in Table 3.3:

Table 3.3. Prestressing forces applied during lifting

Section Type	P_{lift}(kN)			
	C30	C40	C50	C60
I140B120	2358	2856	3314	3743
I160B120	2390	2895	3360	3794
I180B120	2412	2922	3390	3828
I200B120	2425	2938	3409	3849

3.4.4 Cracking tilt angle

In order to simplify the problem, some assumptions are made in the case study. Some values of the relevant parameters are fixed because these constants can be easily changed under different conditions and added to the formula.

- The torsional effect is not considered since the torsional stiffness is larger than the lateral stiffness.
- The inclination angle of the lifting cable is chose to be 0°. Usually, the girders are lifted directly from the top (see Figure 3.7a) or through a rigid steel plate (see Figure 3.7b). In the first way of lifting, the inclination angle of the lifting cable can be chosen to be any value. In the second way of lifting, the inclination angle of the lifting cable can be considered as 0°. If the girder is lifted directly by the cable, the force in the lifting cable will apply on the girder. However, if the girder is lifted through a rigid steel plate, the force in the lifting cable will apply on the plate instead of the girder. Furthermore, since the plate is rigidly connected to the girder, the roll axis will be shifted to the line passing through the loops located on the plate. When the distance between

the center of gravity and roll axis is enlarged, the girder will be more difficult to roll about the axis.

(a). From the top (b). Through a rigid beam

Figure 3.7. Common lifting methods

- The initial eccentricity of the loops e_0 to the center of gravity of the girder is 12 mm.
- The resultant force of the prestress is assumed to be located at the center of the lower flange.
- The loops are located 0.30 m up from the top of the girder, $h_{lift} = 0.30\ m$. In practical, usually this value is larger than 0.20 m. The larger this value is, the more safety factor will be. Here, 0.3m can be seen as an average value and also ensure the safety factor not being overevaluated.

Under all these assumptions and simplifications above, the mathematical expression for calculating the roll angle at cracking stage in equation 3.10 can be simplified to equation 3.15:

$$\theta_{cr} = \left[f_{ctm} - \frac{M_p(h - y_{cg})}{I_{zz}} + \frac{M_{zz,max}(h - y_{cg})}{I_{zz}} + \frac{P_{lift}}{A_c} \right] \times \frac{16 I_{yy}}{q b_1 {l_a}^2} \tag{3.15}$$

3.5 Results

3.5.1. Study cases

After defining all those parameter involved in the physical phenomena, six sets of study cases are established (see Table 3.4) in order to study the influence of different variables on the cracking safety factor FS_{cr}. In each case, some values of the variables are fixed while the others are changeable in order to separate the effects of different parameters on $FS_{cr.}$ Main results regarding the lateral stability behavior of the girder under lifting condition from the cases include the roll angle of the girder at cracking state θ_{cr} and the factor of safety $FS_{cr.}$

Table 3.4. Variables for different cases

Number of cases	l(m)	a(m)	e_i(m)	φ(°)	f	f_{ck}(MPa)
1	40	0	12	0	$l/500$	30,40,50,60
2	40	0	12	0	$l/750$	30,40,50,60
3	20,30,40,50,60	0	12	0	$l/500$	50
4	20,30,40,50,60	0	12	0	$l/750$	50
5	20,30,40,50,60	$l/10$	12	0	$l/500$	50
6	20,30,40,50,60	$l/5$	12	0	$l/500$	50

Comparing the results from different cases, the influences of these variables on θ_{cr} and FS_{cr} can be easily found. For example, from case 1 and 2, the influence of concrete strength f_{ck} on θ_{cr} and FS_{cr} can be obtained. While comparing the results from case 1 and 2 or case 3 and 4, the influence of lateral imperfection f on the behavior can be observed. The results from case 3 or 4 show how θ_{cr} and FS_{cr} vary with the increase of the length of the girder. In case 3, 5 and 6, the influences of the lifting loops' position on the lateral behaviors of the girder are compared by changing the value of a. All the results will be shown in the following part.

3.5.2 Influence of the concrete strength

The roll angle at cracking state θ_{cr} and the factor of safety FS_{cr} derived from case 1 and 2 are summarized in Table 3.5 and Table 3.6. The results are also depicted in terms of I_{zz} in Figures 3.8 - 3.9.

Table 3.5. Roll angles at cracking state

Section Type	*Case 1*				*Case 2*			
	θ_{cr}(°)				θ_{cr}(°)			
	C30	C40	C50	C60	C30	C40	C50	C60
I140B120	10.50	10.57	10.64	10.70	10.50	10.57	10.64	10.70
I160B120	8.69	8.76	8.82	8.88	8.69	8.76	8.82	8.88
I180B120	7.40	7.47	7.53	7.58	7.40	7.47	7.53	7.58
I200B120	6.43	6.49	6.54	6.60	6.43	6.49	6.54	6.60

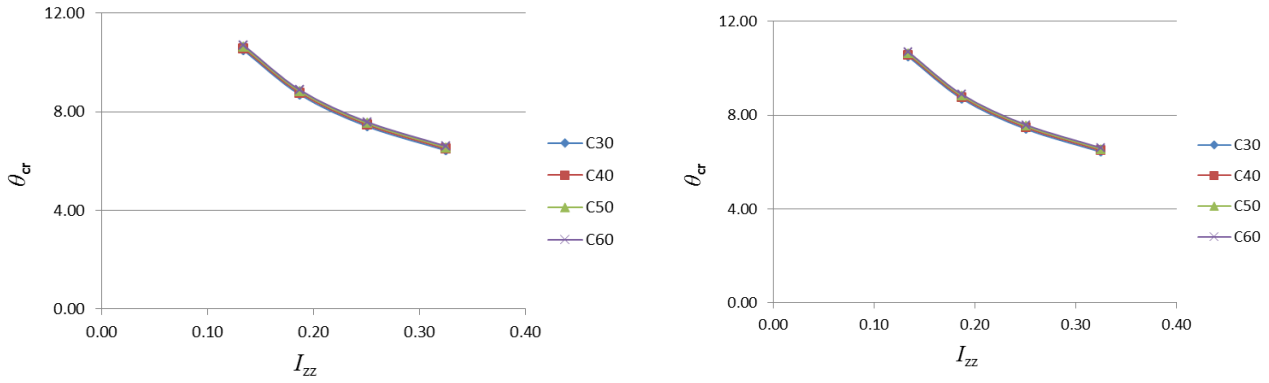

Figure 3.8. θ_{cr} - I_{zz} relationships for different values of f_{ck} : (a) *Case 1* and (b) *Case 2*

From the Table 3.5 and Figure 3.8, it can be concluded that there are no significant differences in the roll angel at cracking state with different concrete strength. This behavior can be proved by using the mathematical expression of θ_{cr} (equation 3.10 or equation 3.15). In those equations, there is only one part that related to f_{ctm}. Since the tensile strengths of the concrete among different strength classes of concrete do not have large differences, these do not play an important role in changing the variation of the cracking roll angles. Furthermore, the curves in Figure 3.8(a) and Figure 3.8(b) show that the roll angle θ_{cr} decreases with the increase of the major inertia of the girder, which means the girder will be more prone to crack with a larger height of the web. The reason for this behavior is that when the height of the girder is increased, the weight of the girder is increased as well, while the lateral inertia is almost constant (I_{yy}/I_{zz} decreases with h).

Table 3.6. Safety factors at cracking state

Section Type	*Case 1*				*Case 2*			
	FS_{cr}				FS_{cr}			
	C30	C40	C50	C60	C30	C40	C50	C60
I140B120	1.23	1.28	1.32	1.35	1.39	1.46	1.51	1.55
I160B120	1.19	1.24	1.28	1.31	1.36	1.43	1.48	1.52
I180B120	1.17	1.22	1.26	1.29	1.34	1.41	1.46	1.51
I200B120	1.15	1.20	1.24	1.27	1.33	1.40	1.45	1.50

Table 3.6 lists the factors of safety with different cross sections against cracking under different concrete strengths. It is clearly that the higher the concrete strength is, the higher the value of FS_{cr} will be. Even though the cracking roll angle do not differ much with different concrete strength classes, the midspan deflection with the full weight z_0 applied on the girder has been changed. The higher the strength of the girder, the lower the value will be. The results present the inverse relations between FS_{cr} and z_0 , which can be also found through the formula. Furthermore, from the figures above it shows that with the same concrete strength, the value of FS_{cr} do not change much with the increase of the depth of the cross section. It can conclude that the safety factor is more

sensitive to the strength of the concrete rather than the height of the cross section.

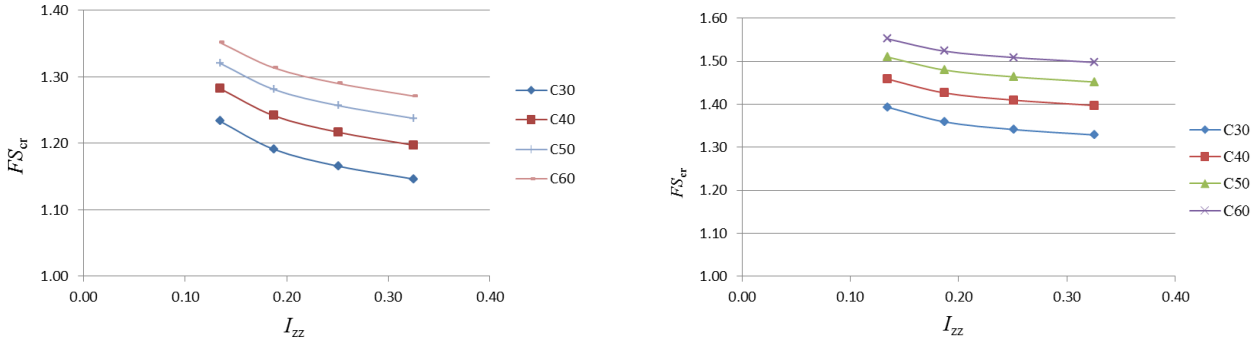

(a) (b)

Figure 3.9. FS_{cr} - I_{zz} relationships for different values of f_{ck} : (a) *Case 1* and (b) *Case 2*

3.5.3 Influence of the length of the girder

The roll angel at cracking state θ_{cr} and the factor of safety FS_{cr} from case 3 and 4 are summarized in Table 3.7 and Table 3.8. The results are also depicted in terms of l from Figure 3.10 to Figure 3.11.

Table 3.7. Roll angles at cracking state

Section Type	*Case 3*					*Case 4*				
	θ_{cr}(degree)					θ_{cr}(degree)				
	l=20	l=30	l=40	l=50	l=60	l=20	l=30	l=40	l=50	l=60
I140B120	12.1	11.0	10.6	10.5	10.4	12.1	11.0	10.6	10.5	10.4
I160B120	10.2	9.2	8.8	8.7	8.6	10.2	9.2	8.8	8.7	8.6
I180B120	8.8	7.9	7.5	7.4	7.3	8.8	7.9	7.5	7.4	7.3
I200B120	7.8	6.9	6.5	6.4	6.3	7.8	6.9	6.5	6.4	6.3

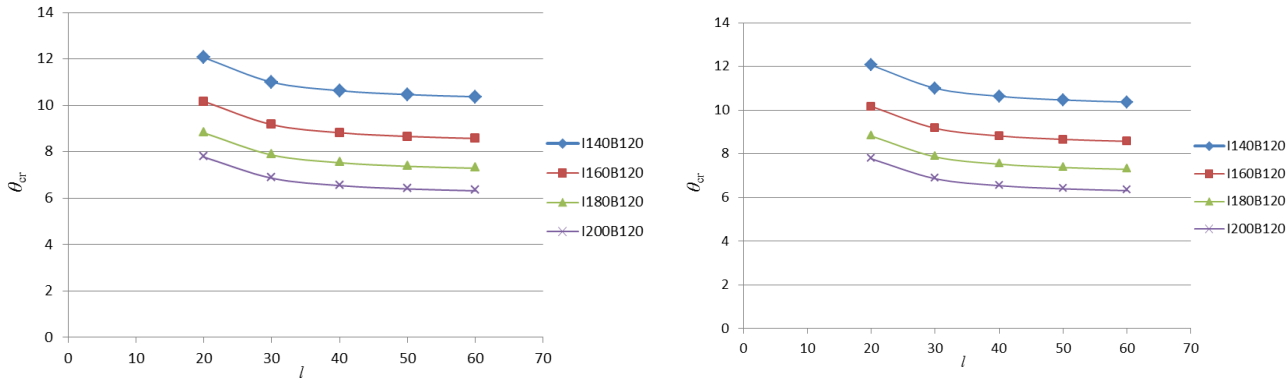

(a) (b)

Figure 3.10 θ_{cr} - l relationships for different cross sections : (a) *Case 3* and (b) *Case 4*

Table 3.8. Safety factors at cracking angles

Section Type	*Case 3*					*Case 4*				
	FS_{cr}					FS_{cr}				
	l=20	l=30	l=40	l=50	l=60	l=20	l=30	l=40	l=50	l=60
I140B120	4.72	2.45	1.32	0.76	0.50	5.92	2.97	1.51	0.83	0.53
I160B120	4.47	2.35	1.28	0.73	0.46	5.61	2.87	1.48	0.81	0.49
I180B120	4.29	2.28	1.26	0.72	0.44	5.40	2.79	1.46	0.80	0.48
I200B120	4.14	2.21	1.24	0.71	0.43	5.23	2.73	1.45	0.80	0.47

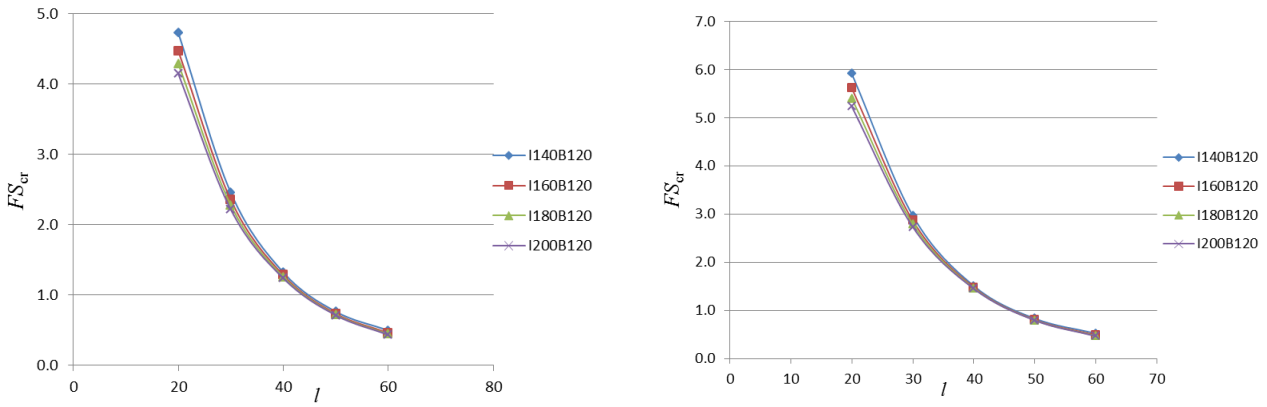

(a) (b)

Figure 3.11 FS_{cr} - l relationships for different cross sections : (a) *Case 3* and (b) *Case 4*

From the curves shown in Figure 3.10(a) and Figure 3.10(b), it is clear that the roll angle decreases with the increase of the length of the girder. In another word, the longer the girder is, the more vulnerable it will be to the lateral instability. It also illustrates the necessity of studying the lateral bending behavior of long-span precast prestressed concrete girder while being lifted. From the curves in Figure 3.11(a) and Figure 3.11(b), the values of FS_{cr} show a sensitive variation to the length of the girder. With all these 4 types of sections, when the length of the girder surpasses a certain value around 40m long, the values of FS_{cr} are lower than 1.0 which are not acceptable and the girder can be seen as unsafe during lifting. The length of the girder plays a significant role in ensuring the lateral stability of the girder while being lifted.

3.5.4 Influence of the lateral imperfection

Both the comparisons between case 1 and 2 or case 3 and 4 have shown that how the values of θ_{cr} and FS_{cr} vary with different initial lateral imperfections. From Table 3.5 and Table 3.7, it is concluded that the roll angle does not change with the variation of lateral imperfection f. This behavior can be easily proved from equation 3.11 where the lateral imperfection does not appear in the expression of cracking roll angle. In another word, the initial lateral imperfection will only cause the initial rigid tilt of the girder, the following lateral bending and deformation of the girder will not be dependent on it. However, the value of the safety factor depends highly on the initial lateral

imperfection. Comparing Figure 3.9(a) and Figure 3.9(b) or Figure 3.11(a) and Figure 3.11(b), the factor of safety is higher with smaller lateral imperfection. The reason can be found through the mathematical expression of FS_{cr}. It is observed from the expression, the lateral imperfection appears in the denominator so that the variation of safety factor is inverse to the variation of lateral imperfection.

3.5.5 Influence of the lifting loops' position

Results from case 3, 5 and 6 show how the lifting loops' position influence the lateral stability of the girder while being lifted. The cracking roll angles from case 5 and 6 are summarized in Table 3.9 and also depicted in Figure 3.12 and Figure 3.13.

Table 3.9. Roll angles at cracking state

Section Type	*Case 5*					*Case 6*				
	θ_{cr}(degree)					θ_{cr}(degree)				
	l=20	l=30	l=40	l=50	l=60	l=20	l=30	l=40	l=50	l=60
I140B120	13.1	11.5	10.9	10.6	10.5	15.4	12.5	11.5	11.0	10.7
I160B120	11.2	9.6	9.1	8.8	8.7	13.4	10.6	9.6	9.2	8.9
I180B120	9.8	8.3	7.8	7.5	7.4	11.9	9.2	8.3	7.9	7.6
I200B120	8.7	7.3	6.8	6.5	6.4	10.7	8.2	7.3	6.9	6.6

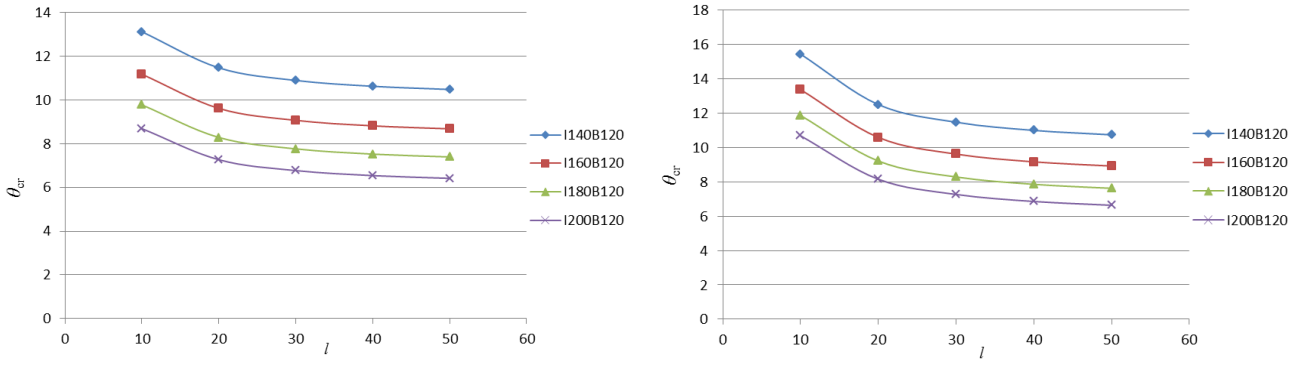

(a) (b)

Figure 3.12 θ_{cr} - l relationships for different cross sections : (a) *Case 5* and (b) *Case 6*

From the table and figures above, it shows obviously that moving the loops inward from the end of the girder can increase the cracking roll angle, which means the resistance of the girder against cracking is increased. The values of FS_{cr} are shown in the following part.

Table 3.10. Safety factors at cracking state

Section Type	*Case 5*					*Case 6*				
	FS_{cr}					FS_{cr}				
	l=20	*l*=30	*l*=40	*l*=50	*l*=60	*l*=20	*l*=30	*l*=40	*l*=50	*l*=60
I140B120	7.212	4.289	2.764	1.873	1.370	8.90	5.46	4.08	3.44	3.22
I160B120	6.835	4.047	2.613	1.753	1.243	8.54	5.12	3.76	3.08	2.76
I180B120	6.578	3.876	2.511	1.680	1.171	8.31	4.89	3.54	2.85	2.48
I200B120	6.382	3.741	2.431	1.628	1.125	8.15	4.72	3.38	2.68	2.29

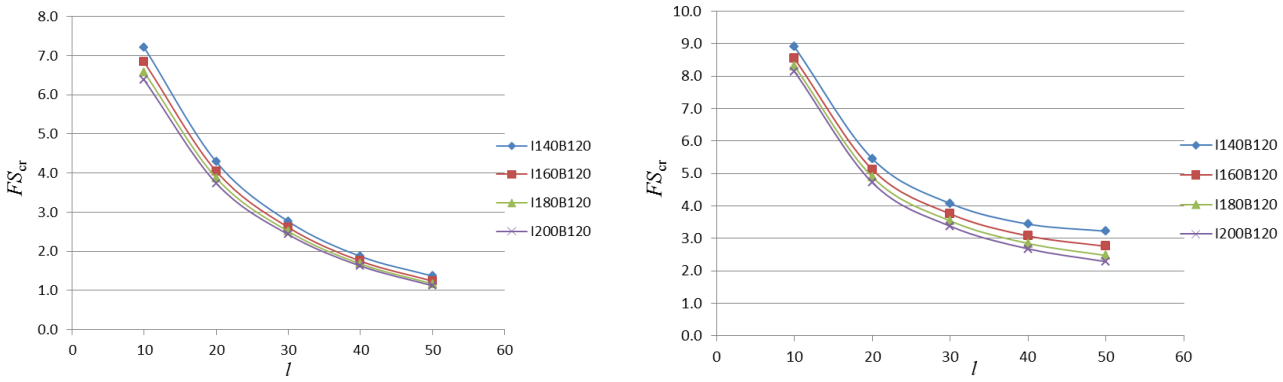

(a) (b)

Figure 3.13 FS_{cr} - *l* relationships for different cross sections : (a) *Case 5* and (b) *Case 6*

The results from above also show the positive effects of moving the loops inward on the safety factor. It verifies the theory from Anderson (1971) and Imper and Laszlo (1987) given in Chapter 2.

CHAPTER 4.

NEW PROPOSED APPROACH FOR CODE PROVISION

4.1 INTRODUCTION

The main goal of this research is to propose a simplified formula which can be applied by practitioners to check and design for lateral stability of precast prestressed girders during lifting operations. The should include the most sensitivity and representative design parameters which can be predefined such as the properties of the material and the cross-section. In Chapter 3, the physical-analytical model has been introduced and the effects of the main parameters on the FS_{cr} have been analyzed. However, the resulting equation (equation 3.11) is still large and requires numerical tools to be solved. It is not convenient for designers to verify whether the girder is safe or not to be lifted by using this method.

Thus, in the following chapter, closed formulas will be proposed which will be valid under certain assumptions, these being general and cover the vast majority of the cases. Two main formulas are mainly considered in the following: (1) the formula of cracking roll angle θ_{cr} and (2) the formula of the safety factor FS_{cr}. A real study case of a bridge long precast prestressed concrete girder which failed during lifting operations will be checked by considering the provisions gathered in the main structural design codes and the closed formula proposed herein.

4.2 PROPOSED CLOSED FORMULA

4.2.1 Main assumptions

- The lifting loops are assumed to be located at the end of the girder$(a = 0)$. From the results in Chapter 3, moving the lifting loops inward from the end will increase the capacity of the beam against the lateral failure. Not only will the results under this assumption be on the safe side, but also simplify the calculation. The midspan lateral deflection with all the self-weight applied has been simplified as:

$$z_0 = \frac{qA_c}{120EI_{yy}} \tag{4.1}$$

Here, the modulus of the concrete can be expressed in terms of the characteristic compressive strength of the concrete (f_{ck}) as:

$$\mathrm{E} = 8500\sqrt[3]{f_{ck} + 8} \tag{4.2}$$

- The center of gravity of the section is assumed to be at the half height of the cross-section. This assumption is concluded from the example sections used for the experiments before.Moreover, symmetrical I-sections are also commonly used in projects. Thus, the distance between the center of gravity and the lifting loops y_r can be simplified as:

$$y_r = \frac{h}{2} + h_{lift} - \delta_G \tag{4.3}$$

Under this assumption, the eccentricity of the resultant prestressing force to the center of gravity of the section is:

$$e_p = \frac{h - h_3}{2} \tag{4.4}$$

Usually, the precamber of the beam results from the prestressing force can be determined by the prefabricated company and the maximum value of it is usually less than 0.10 m.

- The initial eccentricity of the loops from the center is not considered in the simplified FS_{cr} formula since it is usually much smaller compared to other parameters.

4.2.2 Proposed simplified formulas

Under all the assumptions made, the simplified formulas for assessing the cracking roll angle θ_{cr} and the factor of safety FS_{cr} can be expressed as equation 4.5 and 4.6 respectively The detail of deduction can be found in Appendix X.

$$\theta_{cr} = 0.0288 \frac{(f_{ck})^{2/3} I_{yy}}{b_1 A_c l^2} + \frac{h I_{yy}}{b_1 I_{zz}} \tag{4.5}$$

$$\mathrm{FS}_{cr} = \frac{h - y_{cg} + y_{lift} - \delta_G}{\frac{A_c l^4}{40800 \times 10^3 I_{yy} {f_{ck}}^{1/3}} \left(1 + 2.72 \times 10^7 \frac{f b_1 I_{zz} {f_{ck}}^{1/3}}{h A_c l^4}\right)} \tag{4.6}$$

For lateral imperfection $l/500$, the FS_{cr} can be calculated by equation 4.7:

$$\mathrm{FS}_{cr} = \frac{h - y_{cg} + y_{lift} - \delta_G}{\frac{A_c l^4}{40800 \times 10^3 I_{yy} {f_{ck}}^{1/3}} \left(1 + 54.4 \times 10^3 \frac{b_1 I_{zz} {f_{ck}}^{1/3}}{h A_c l^3}\right)} \tag{4.7}$$

For lateral imperfection $l/750$, the formula is changed to equation 4.8:

$$\mathrm{FS}_{cr} = \frac{h - y_{cg} + y_{lift} - \delta_G}{\frac{A_c l^4}{40800 \times 10^3 I_{yy} {f_{ck}}^{1/3}} \left(1 + 36.27 \times 10^3 \frac{b_1 I_{zz} {f_{ck}}^{1/3}}{h A_c l^3}\right)} \tag{4.8}$$

In the formulas above, y_{lift} and δ_G are usually determined by the precast company, or fixed by the designer. In the final proposed formulas, these two parameters are assumed with a value of 0.0, which will ensure the results to be on the safe side.

For lateral imperfection $l/500$, the FS_{cr} can be calculated by equation 4.9:

$$\mathrm{FS}_{cr} = \frac{\frac{h}{2}}{\frac{A_c l^4}{40800 \times 10^3 I_{yy} {f_{ck}}^{1/3}}\left(1 + 54.4 \times 10^3 \frac{b_1 I_{zz} {f_{ck}}^{1/3}}{h A_c l^3}\right)} \tag{4.9}$$

For lateral imperfection $l/750$, the formula is changed to equation 4.10:

$$\mathrm{FS}_{cr} = \frac{\frac{h}{2}}{\frac{A_c l^4}{40800 \times 10^3 I_{yy} {f_{ck}}^{1/3}}\left(1 + 36.27 \times 10^3 \frac{b_1 I_{zz} {f_{ck}}^{1/3}}{h A_c l^3}\right)} \tag{4.10}$$

4.2.3 Verification of the formulas with the results from the experiments

The main idea of proposing the formulas above is to build relations between the two unknown variables, which are θ_{cr} and FS_{cr}, and the basic properties of the materials and cross sections. The more important result for designers would be the value of FS_{cr}. The comparison of the results from case 1 by using both Mast model and proposed formulas are shown as follows.

Table 4.1 and Table 4.2 show the cracking roll angle from both models with case 1. Figure 4.1 and Figure 4.2 plot the curves from both models.

Table 4.1. Roll angles at cracking state with different models (case 1)

Section Type	θ_{cr}**(degree)** *Mast's Model*				θ_{cr}**(degree)** *Proposed Model*			
	C30	C40	C50	C60	C30	C40	C50	C60
I140B120	10.50	10.57	10.64	10.70	10.51	10.59	10.65	10.71
I160B120	8.69	8.76	8.82	8.88	8.65	8.72	8.78	8.84
I180B120	7.40	7.47	7.53	7.58	7.34	7.40	7.46	7.52
I200B120	6.43	6.49	6.54	6.60	6.34	6.40	6.46	6.51

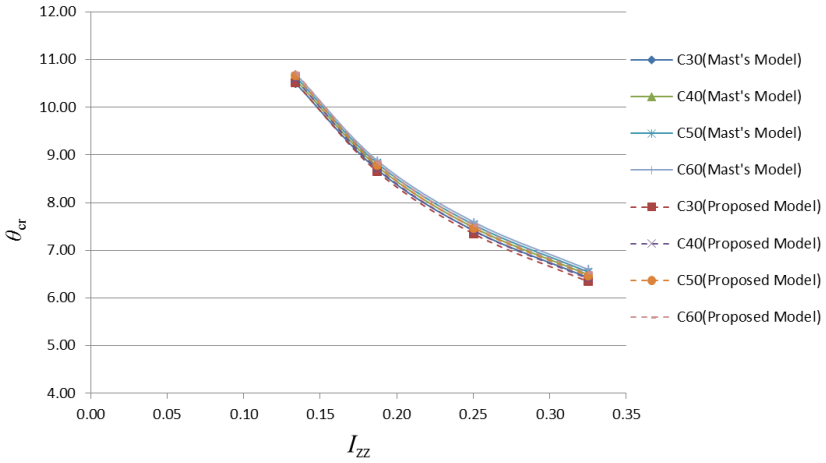

Figure 4.1. Roll angles at cracking state with different models (case 1)

Table 4.2. Safety factors at cracking state with different models (case 1)

Section Type	***FS*cr *Mast's Model***				***FS*cr *Proposed Model***			
	C30	C40	C50	C60	C30	C40	C50	C60
I140B120	0.91	0.97	1.01	1.05	0.89	0.94	0.98	1.02
I160B120	0.93	0.99	1.03	1.07	0.90	0.96	1.00	1.03
I180B120	0.95	1.01	1.06	1.09	0.92	0.97	1.01	1.04
I200B120	0.97	1.03	1.07	1.11	0.93	0.98	1.01	1.04

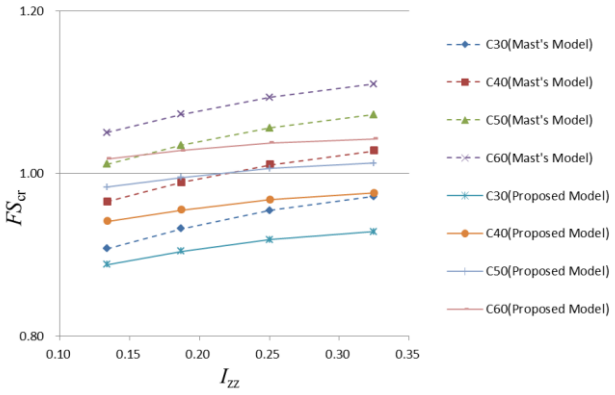

Figure 4.2. Safety factors at cracking state with different models (case 1)

The results confirm that the proposed model leads to values of θ_{cr} and FS_{cr} on the safe side for all the cases, the average error being 1.0% and 5.0% for θ_{cr} and FS_{cr}, respectively, comparing with the Mast model. Above all, the proposed model can be considered acceptance to evaluate the lateral safety of the girder while being lifted.

4.3 STUDY OF THE PROPOSED MODEL WITH SECTIONS FROM AASHTO

In order to spread the application of the formulas proposed above, typical standard AASHTO *I*-beams from PCI bridge design manual are studied in this part. (Bridge Design Manual, 2011). The shape of the cross section is depicted in Figure 4.3. Some properties of the beam are listed in Table 4.3.

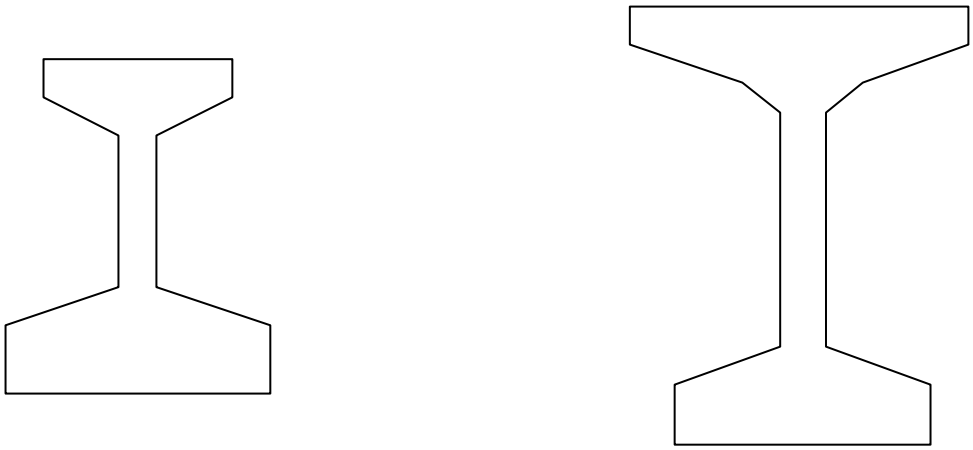

(a). Shape of cross section type Ⅰ, Ⅱ, Ⅲ, Ⅳ (b). Shape of cross section type Ⅴ, Ⅵ

Figure 4.3. Shape of cross secions from AASHTO

Table 4.3. Physical properties of the cross sections in AASHTO

Section Type	b_1(m)	h(m)	A_c(m2)	I_{zz}(m^4)	I_{yy}(m^4)	y_{cg}(m)	e_p(m)
Ⅰ	0.30	0.71	0.18	0.01	0.00	0.32	0.17
Ⅱ	0.31	0.91	0.24	0.02	0.00	0.40	0.22
Ⅲ	0.41	1.14	0.36	0.05	0.01	0.51	0.31
Ⅳ	0.51	1.37	0.51	0.11	0.01	0.63	0.40
Ⅴ	1.07	1.60	0.65	0.22	0.03	0.81	0.44
Ⅵ	1.07	1.83	0.70	0.31	0.03	0.92	0.39

Provided that the factor of safety FS_{cr} is 1.0, the maximum length of the girder for each type of section with different strength of concrete can be found by equation 4.8. The basic assumptions for this study are:

- The lateral imperfection is $l/500$
- y_{lift} and δ_G are neglected

The results are shown as follows in Table 4.4.

Table 4.4. Maximum length of the girder by keeping $FS_{cr} = 1.0$

Section Type	Maximum length(m)			
	C30	C40	C50	C60
Ⅰ	23.93	24.47	24.90	25.25
Ⅱ	26.91	27.52	28.00	28.40
Ⅲ	31.29	32.00	32.55	33.02
Ⅳ	35.56	36.36	37.00	37.52
Ⅴ	42.26	43.17	43.89	44.48
Ⅵ	42.66	43.56	44.28	44.87

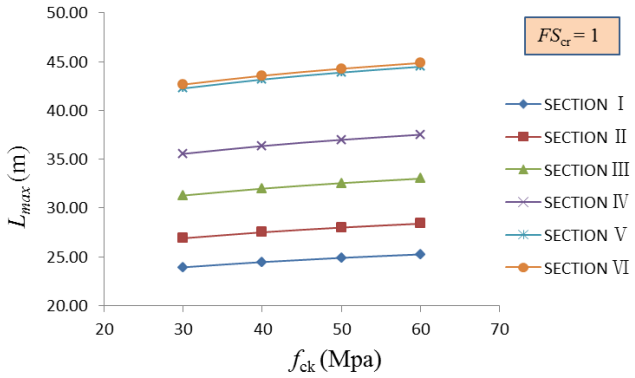

Figure 4.4. Maximum length of the girder by keeping $FS_{cr} = 1.0$

Some conclusions can be drawn from the results.

- The higher the concrete strength is, the larger the maximum length for the beam will be.
- From section Ⅰ to section Ⅳ, even though the major inertia of the section is increased, the minor inertia of the section remains almost the same. However, the minor inertias of section Ⅴ and section Ⅵ have been increased significantly from the previous four sections, which present a significant increase in the safety factor as well. Comparing the results for section Ⅴ and section Ⅵ, the safety factor does not change much with the major inertia when the minor inertia remains the same.

Another analysis has also been carried out with these sections. This analysis aims to discover the increment of the girder's length with different initial lateral imperfections respect to no lateral imperfections. 3 cases are tested with a concrete strength C30.

Above all, the smaller the lateral imperfection is, the larger the length of a girder could have. It has to be pointed out that the results in Table 4.5 without any lateral imperfection represent the maximum length for near perfect beams. To put it into another way, in order to ensure the lateral stability of the girder under lifting, the length of a

particular girder with any lateral imperfection cannot surpass the one without any imperfection. This is also explained in Mast's work (Mast, 1989). He defined a critical safety factor which is based on a near perfect girder without lateral imperfection. He pointed out that the roll angle with no imperfection is also the maximum angle a girder can reach. Beams with initial imperfections would fail before reaching this point. So that the safety factor for other cases should be larger than the one without imperfection.

Table 4.5. Maximum length of the girder by keeping $FS_{cr} = 1.0$ with different initial lateral imperfections

Section Type	**Maximum Length (m)**			
	0	*l*/1000	*l*/750	*l*/500
I	25.46	24.71	24.45	23.93
II	28.51	27.72	27.45	26.91
III	33.30	32.31	31.97	31.29
IV	37.95	36.77	36.37	35.56
V	46.74	44.55	43.80	42.26
VI	47.63	45.20	44.36	42.66

Table 4.6. Variation of the maximum length of the girder by keeping $FS_{cr} = 1.0$ with different initial lateral imperfections

Section Type	**Δ*l*/*l* (%)**			
	0	*l*/1000	*l*/750	*l*/500
I	0.00	-2.96	-3.97	-6.01
II	0.00	-2.77	-3.70	-5.60
III	0.00	-2.98	-3.99	-6.05
IV	0.00	-3.10	-4.15	-6.29
V	0.00	-4.68	-6.29	-9.57
VI	0.00	-5.10	-6.85	-10.43

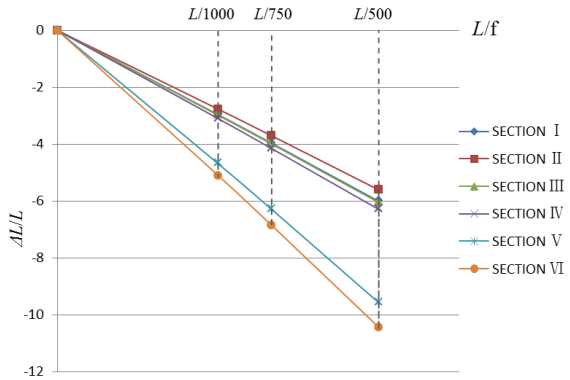

Figure 4.5. Variation of the maximum length of the girder by keeping $FS_{cr} = 1.0$ with different initial lateral imperfections

4.4 STUDY CASES

In order to demonstrate the reliability of the proposed model in real project, a real failure case has been studied in this part. This example will be examined by different provisions in several codes to verify its possibility of failure and the reliability of the limitations in different codes regarding the lateral instability problem for long precast prestressed beam during lifting.

This real failure case occurs during the construction of a viaduct near Olost, Catalonia, Spain. The precast prestressed concrete girder is 45.6m in length with an I-shaped cross section (see Figure 4.6). It was lifted by two cables in vertical at a distance of 2m from the end of the girder and 0.3m up from the top of the girder at site. The girder has an area of 0.58m^2, a depth of 2m, a major inertia of 0.324m^4 and a minor inertia of 0.02m^4 of the cross section, respectively. The prestressing force applied on the girder when it was lifted was around 8514kN (considering 15% loss) with an eccentricity of 0.73m from the center of gravity of the cross section. The compressive strength of the concrete during construction was 60N/mm^2 at 28days. A eccentricity of 12mm of the lifting loops from the central axis was considered and a total sweep (lateral imperfection) of 90mm ($l/510 < l/500$ allowed by EN 15050:2008) was measured before lifting. Thus the lifting operation was confirmed by the supervisor.

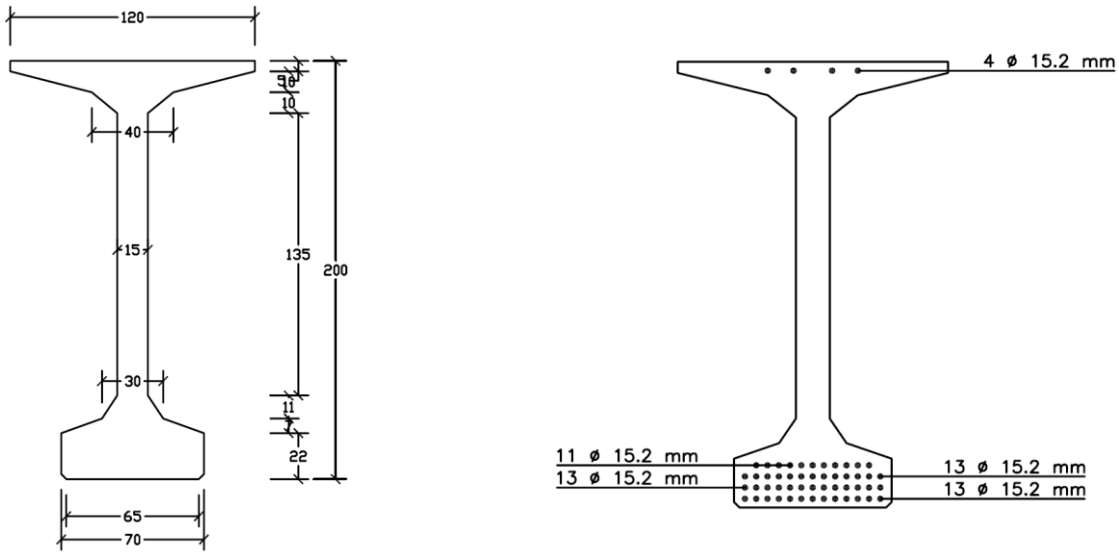

Figure 4.6. Dimensions (cm) and active reinforcement of the cross section.

However, during lifting a significant lateral deflection (around 300mm) was observed (see Figure 4.7a). Some vertical cracks were also observed at the left upper flange (where appears the maximum tensile stresses in this particular case). The technician then decided to lowdown the girder to examine the possibility of failure (see Figure 4.7b) and then tried the second time. However, in the second time of lifting after the girder was placed over

the beating pads of the pillars of the bridge, it presented a lateral deflection of more than $l/400$ (see Figure 4.7c) and was unable to be recovered to the original shape. Therefore, a new girder was manufactured again and transported to the site to replace the failure one. There was no any problem with the second girder with an initial lateral imperfection of $l/590$.

(a)

(b)

(c)

Figure 4.7. First lifting operation (a), deformed shape after first lifting (b) and deformed shape once in place after second lifting (b).

By using all the information provided above, the possibilities of failure in this case evaluated by different provisions in different codes or guidelines are shown below in Table. xx. The proposed model is also used to examine the potential failure of the girder. Provisions in EHE-08 and the proposed model are the only two which the outcomes from the case are not fulfilled. This indicates that the provisions for preventing the lateral instability during lifting stage in other codes are not credible in this specific case.

Table 4.7. Provisions from codes and guidelines to prevent lateral instability and values for case study

Code or guideline	Recomendation	Value for real case study	Conclusion
EN 15050:2008	$e_i \leq \frac{l}{500}$	$e_i = \frac{l}{510}$	Fulfilled (unsafe)
Eurocode 2*	$\frac{l}{b} \leq \frac{70}{(h/b)^{\frac{1}{3}}}$	$38 \leq 59$	Fulfilled (unsafe)
	$\frac{h}{b} \leq 3.5$	$1.7 \leq 3.5$	Fulfilled (unsafe)
fib Model Code 2010*	$\frac{l}{b} \leq \frac{50}{(h/b)^{\frac{1}{3}}}$	$38 \leq 42$	Fulfilled (unsafe)
ACI 318-08*	$\frac{l}{b} \leq 50$	$38 \leq 50$	Fulfilled (unsafe)
PCI 2016	$FS_{cr} \geq 1.00$	$1.07 \geq 1.00$	Fulfilled (unsafe)
ABNT NBR 6118	$\frac{h}{b} \leq 2.5$	$1.67 < 2.5$	Fulfilled (unsafe)
	$\frac{l}{b} \leq 50$	$38 \leq 50$	Fulfilled (unsafe)
BS:8110-1	$\frac{lh}{b^2} \leq 250$	$63.3 < 250$	Fulfilled (unsafe)
	$\frac{l}{b} \leq 60$	$38 \leq 60$	Fulfilled (unsafe)
JTG D62-2004	$l \leq 50$	$45.6 \leq 50$	Fulfilled (unsafe)
Spanish Code EHE-08 (Annex 11)	$e_i \leq \frac{l}{750}$	$e_i = \frac{l}{510}$	Not fulfilled (safe)
Proposed model	$FS_{cr} \geq 1.00$	$0.76 \leq 1.00$	Not fulfilled (safe)
* ***b*** and ***h*** being the width of the upper flange and h the height of the cross section, respectively			

CHAPTER 5.

CONCLUSIONS AND FUTURE RESEARCHES

5.1 SUMMARY OF THE RESEARCH

First of all, this research discusses the importance of the lateral stability of long span precast prestressed concrete girders during lifting stage at sites. Different models studied on this problem from other previous researches are compared. Meanwhile, provisions in current standards and codes regarding lateral instability are summarized. Though the torsional and lateral bending behaviors were deeply studied for preventing potential failure, accidents happened due to lateral instability. This has arouse the attention to build up a new models and further research.

In the second part of this research work, a parametric study has been carried out with the help of a proposed numerical model in Matlab. Critical state in this problem is predefined based on the stress state against cracking and recommendations gathered in the PCI Bridge Design Handbook. The inputs of this study include physical properties of cross sections, strength of materials and boundary conditions of the girder to be designed. The cross sections chosen for this study are from a commercial girder catalogue. The outputs of the analysis include the roll angle and the cracking safety factor. The main aim of this parametric study is to figure out how the inputs affect the behavior of the girder in terms of the roll angle and safety factor.

Finally, based on the numerical model and the results derived from the parametric study, new approach for assessing the lateral stability of long span precast prestressed concrete girders is proposed. Those parameters which were proven to show less sensitiveness in the parametric study were neglected in the final formulas. The proposed formulas are applied to one of the case study from the previous part and the results highly coincide with those from the full numerical model. Furthermore, a real case failed during lifting is analyzed by the new approach, which gives the recommendation if the girder is of sufficient lateral stability according to this approach. Meanwhile, recommendations from current standards are also listed and compared in order to show their reliability of evaluating the lateral stability of the girder.

5.2 CONCLUSIONS

1. Current standards only take into account some dimensions of the section and beam length. This study has proven that parameters such as Young Modulus, precamber and concrete strength govern the stability problem and could be of paramount importance.

2. The model proposed here in lead to results from the safety side while is capable of considering the main governing parameters.

3. The width of the upper flange has a negative influence of the lateral stability.

It should be highlighted that this research will be summarized and presented in the *fib* TC 6.5 Precast Concrete Bridges in which new provisions are being developed for a future bulletin expected to be realized in 2018. Likewise, the author of this Master Thesis will promote the acceptance of the proposed equation for the Chinese Code, since no provisions are gathered in this regulation nowadays.

5.3 RECOMMENDATIONS

Some recommendations for improving the lateral stability of the long span precast prestressed girders can be drawn from the previous studies.

- The most efficient way to improve the lateral stability of long span precast prestressed concrete beam during lifting would be moving lifting positions inward from the ends of the girder. Not only because the lateral deflection is reduced by almost fourth power of the net span, but also because the end blocks have a positive effect on the bending behavior of the girder. Results from case 3, 5 and 6 in parametric study show this trend. However, due to some design constraints, the lifting points cannot be moved inward as much as possible. The most practical and economical distance would be 1/10*l* from the ends.
- Due to the demanding of design and construction, the length of the precast prestressed girders has been increased significantly in many projects. In order to decrease the deflection and deformation of the girder, the most common way is to increase the height of the cross section which will increase the major inertia as well. However, the minor inertia almost remains constant and the girder is more vulnerable to lateral failure since the weight of the beam is increased. It is necessary to increase both the major and minor inertia of the girder. It could be done by increasing the height of the cross section as well as the width of the flanges.
- It has to be pointed out that the lower flange contributes as much as the upper flange in preventing potential failure in lateral bending of girders during lifting stage. Adding material to the bottom flange have many benefits on improving lateral stability of the girder. Firstly, it will lower the center of gravity of the girder, which will increase the resisting moment against rolling about the axis. Secondly, the moment caused by the prestressing force will be decreased, which means the tensile stress of the critical point on the cross section will be decreased as well. Thirdly, the weak-axis stiffness will be increased by adding materials to the flange.
- The safety factor against cracking can be improved by higher concrete strength. Girders with higher concrete strength will have higher bending stiffness both in strong-axis and weak-axis. What is more, the girder would be more difficult to crack with higher tensile strength. `
- It is better to lift the long beams with length larger than 40 meters at *l*/10 or *l*/5 from the ends.

5.4 FUTURE RESEARCH

Though the method proposed in this paper may be valid to evaluate the lateral stability of long span precast prestressed concrete girders hanging from lifting loops, it has to be extended to more general situations. Since the lack of sufficient lateral restraints in both transport and lifting cases, girders tend to roll sideways and produce lateral bending of the beam. Therefore, the lateral stability of such girders during transport would be another critical state to be controlled by the construction personnel. Mast had carried out similar analysis of such girders supported from below, which refers to the transport phase (Mast, 1993). Hurff and Kahn had also conducted an experimental study on rollover stability of prestressed concrete girders on flexible bearings (Hurff and Kahn, 2012). The differences between transport and lifting cases would be the support type. In transport case, girders are usually located on elastic supports which could be deformed along with the girder. Studies on the behavior of those supports would be a key point in the future research. What is more, some non-linear analysis related to the lateral

stability would also be expected since the properties of the support and the post-cracking properties of girders may be nonlinear (Mast, 1993). Effective method on evaluating the potential failure of long span precast prestressed concrete girders would be proposed in the future study.

References

ACI Committee 318, "Building Code Requirements for Structural Concrete (ACI 318-02) and Commentary (318R-02)," American Institute, Farmington Hills, Michigan, 2002, 443 pp.

Anderson, A. R. "Lateral stability of long prestressed concrete beams". PCI Journal, 16(3), 7-9. May-June 1971.

Castrodale, R. W. and White, C. D. "Extending Span Ranges of Precast Prestressed Concrete Girders". National Cooperative Highway Research Program, Report 517. Washington D. C., 2004.

Code for Design of highway Reinforced Concrete and Prestressed Concrete Bridges and Culverts (JTG D62-2004), 2004.

Cojocaru, R. (2012) "Lifting Analysis of Precast Prestressed Concrete Beams". Virginia Polytechnic Institute and State University, Master of Science in Civil Engineering.

EHE-08. Comisión Permanente del Hormigón. Instrucción de Hormigón Estructural. Ministerio de Fomento. 3th Edition, 2009.

EN 15050:2008 +A1:2012. Precast concrete products – Bridge elements.

Eurocode 2: Design of Concrete Structures. Technical Sector Board for Building and Civil Engineering, 1999.

fib Bulletins 65-66, Model Code 2010. Final Draft, 2010. fédération internationale du béton (fib), Lausanne, Switzerland.

Hurff, J. "Stability of Precast Prestressed Concrete Bridge Girders Considering Imperfections and Thermal Effects". Georgia Institute of Technology, School of Civil and Environmental Engineering, August 2010.

Imper, R.R., Laszlo, G. (1987). *Handling and Shipping of Long Span Bridge Beams*. PCI journal, 32(6).

Laszlo, G. and Imper, R. R. "Handling and Shipping of Long Span Bridge Beams". PCI Journal, November-December 1987, pp. 86-101.

Marrey, B. and Grote, J. "The story of prestressed concrete from 1930 to 1945: A step towards the European Union". Proceedings of the First International Congress on Construction History. Madrid, January, 2003.

Mast, R. F. (1989). "Lateral Stability of Long Prestressed Concrete Beams, Part 1." PCI J. 34(1), 34–53.

Mast, R. F. (1993). "Lateral Stability of Long Prestressed Concrete Beams, Part 2." PCI Journal., 38(1), 70–88.

Mast, R. F. (1994). "Lateral bending test to destruction of a 149 ft. prestressed concrete I-beam." PCI J., 39(1), 54-62.
Muller, J. "Lateral Stability of Precast Members During Handling and Placing". PCI Journal, February 1962, pp. 20-31.

PCI *Design handbook*. 1st ed. Chicago: Precast/Prestressed Concrete Institute. 1992

PCI *Recommended Practice for Lateral Stability of Precast, Prestressed Concrete Bridge Girders*, Chicago, IL. 2016

PCI. *Recommended practice for lateral stability of precast, prestressed concrete bridge girders* (CB-02-16). PCI committee on Bridges. 2016.

Peart, W.L., Rhomberg, E.J., James, R.W. (1992). Blucking of suspended camber girders. ASCE J Struct. Eng. 118(2): 505-528.

Plaut, R. H., Moen, C. D. (2013). "Analysis of elastic, doubly symmetric, horizontally curved beams during lifting." J. Struct. Eng., 139(1), 39-46.

Plaut, R. H., Moen, C. D. (2014). "Stability of unbraced concrete beams on bearing pads including wind loading." Eng. Struct., 69, 246-254.

Plaut, R. H., Moen, C. D., Cojocaru, R. (2012). "Beam deflections and stresses during lifting." Eng. J.., 49(4), 187-194.

Stratford, T.J., Burgoyne, C. J. (1999a). "Lateral stability of long precast concrete beams". Proc. Instn Civ. Engrs Structures & Bldgs, May-August 1999, 124, pp. 169-180.

Swann, R. A., Readers comment to "Lateral Stability of Long Prestressed Concrete Beams", PCI Journal, 16(6), November-December 1971.

Technical Specifications for Highway Bridges and Culverts (JTJ041-2000), China, 2000.

Timoshenko, S., and Gere, J. (1961). *Theory of elastic stability*. McGraw-Hill Book Co., New York, N.Y.
Troyano, L.F.: "Bridge Engineering - A Global Perspective", Thomas Telford Publishing, 2003.

Victor, H. (2015). "Lateral stability analysis of long precast prestressed concrete beams". Master thesis, Universitat Politècnica de Catalunya.

Yegian, S. (1956). "Lateral buckling of I beams supported by cables." Ph.D.thesis, Univ. of Illinois, Urbana, IL.